# Comprehensive lipidomic analysis of human plasma using multidimensional liquid- and gas-phase separations: Two-dimensional liquid chromatography-mass spectrometry vs. liquid chromatography-trapped-ion-mobility-mass spectrometry

Baglai, A.; Gargano, A.F.G.; Jordens, J.; Mengerink, Y.; Honing, M.; van der Wal, S.; Schoenmakers, P.J.

**DOI**
10.1016/j.chroma.2017.11.014

**Publication date**
2017

**Document Version**
Final published version

**Published in**
Journal of Chromatography A

Journal of Chromatography A, 1530 (2017) 90–103

Contents lists available at ScienceDirect

Journal of Chromatography A

journal homepage: www.elsevier.com/locate/chroma

Full length article

# Comprehensive lipidomic analysis of human plasma using multidimensional liquid- and gas-phase separations: Two-dimensional liquid chromatography–mass spectrometry *vs.* liquid chromatography–trapped-ion-mobility–mass spectrometry

Anna Baglai[a,b,*], Andrea F.G. Gargano[a,b], Jan Jordens[c], Ynze Mengerink[c], Maarten Honing[c,d], Sjoerd van der Wal[b], Peter J. Schoenmakers[b]

[a] TI-COAST, Science Park 904, 1098 XH Amsterdam, The Netherlands
[b] University of Amsterdam, Van't Hoff Institute for Molecular Sciences, Science Park 904, 1098 XH Amsterdam, The Netherlands
[c] DSM Resolve, Urmonderbaan 22, 6167 RD, Geleen, The Netherlands
[d] Division of BioAnalytical Chemistry, Vrije Universiteit, De Boelelaan 1083, 1081 HV Amsterdam, The Netherlands

ARTICLE INFO

*Article history:*
Received 1 June 2017
Received in revised form 6 November 2017
Accepted 9 November 2017
Available online 10 November 2017

*Keywords:*
Lipidomics
Multidimensional separation
Trapped-ion-mobility–mass spectrometry
On-line comprehensive two-dimensional liquid chromatography
Human plasma
Untargeted analysis

ABSTRACT

Recent advancements in separation science have resulted in the commercialization of multidimensional separation systems that provide higher peak capacities and, hence, enable a more-detailed characterization of complex mixtures. In particular, two powerful analytical tools are increasingly used by analytical scientists, namely online comprehensive two-dimensional liquid chromatography (LC × LC, having a second-dimension separation in the liquid phase) and liquid chromatography-ion mobility-spectrometry (LC-IMS, second dimension separation in the gas phase).

The goal of the current study was a general assessment of the liquid-chromatography–trapped-ion-mobility–mass spectrometry (LC-TIMS–MS) and comprehensive two-dimensional liquid chromatography–mass spectrometry (LC × LC–MS) platforms for untargeted lipid mapping in human plasma.

For the first time trapped-ion-mobility spectrometry (TIMS) was employed for the separation of the major lipid classes and ion-mobility-derived collision-cross-section values were determined for a number of lipid standards. The general effects of a number of influencing parameters have been inspected and possible directions for improvements are discussed.

We aimed to provide a general indication and practical guidelines for the analyst to choose an efficient multidimensional separation platform according to the particular requirements of the application. Analysis time, orthogonality, peak capacity, and an indicative measure for the resolving power are discussed as main characteristics for multidimensional separation systems.



## 1. Introduction

One of the most complex and challenging research areas for modern analytical chemistry is metabolomics. The aim of metabolomics investigations is to trace changes in the chemical and biochemical compositions of all metabolites present in biological fluids and tissues. Lipidomics is a relatively young branch of metabolomics, which aims to characterize the complexity of lipids in biological matrixes. Lipids were found to be involved in biochemical processes, cell functions and structures, and signalling changes related to human health [1–3]. Therefore, a comprehensive analysis of lipids is gaining increased attention. This development is reinforced by recent advancements in separation technology.

The objective in untargeted analysis is to gain as much information and insight in sample composition as possible. The typical analysis platform used to resolve the high diversity of lipid species is liquid chromatography (LC) coupled to high-resolution mass spectrometry (HRMS) [4–7]. However, in lipid samples many isobaric compounds are present, which show a high tendency to co-elute. Co-eluting compounds have potentially very different structures and ionization efficiencies, and they may occur in very

* Corresponding author at: TI-COAST, Science Park 904, 1098 XH Amsterdam, The Netherlands.
*E-mail addresses:* a.baglai@uva.nl, anna.baglai@gmail.com (A. Baglai).

https://doi.org/10.1016/j.chroma.2017.11.014
0021-9673/

different concentrations. This results in the suppression of low-abundance species in the ionization chamber of the MS. As a result, LC–MS, despite the great resolution and mass accuracy, will generally lead to loss of biologically important information in the characterization of lipid samples. Therefore, lipidomics analysis requires the combination of several platforms.

During the last decade, ion-mobility spectrometry (IMS) has proven to be a versatile technique for lipidomic analysis [8–11]. In ion mobility, molecules are separated in the gas-phase according to their charge, size and shape in the presence of neutral gas. The parameters are reflected in characteristic mobilities ($K$). From the analyte mobility a specific physicochemical ion parameter – the collisional cross-section area (CCS) – can be calculated. This may be used for compound characterization and identification, akin to $m/z$ values in mass-spectrometry.

Coupling of IMS with a liquid chromatography–mass spectrometry (LC–MS) system provides an additional (third) dimension. Because the timescale of chromatographic separation (LC) is in minutes and that of mass-spectrometry (MS) is in microseconds, a rapid gas-phase separation, such as IMS with its millisecond timeframe, can be incorporated time-independently between LC and MS, resulting in increased specificity of lipids identification.

Because of its high resolution power the combined LC-IMS–MS approach facilitates targeted lipid analysis for structural elucidation [9,12–14], isomer separation within a specific lipid class [5,15–18], determining positions of double-bonds in the fatty acyl chains [19], and the general separation of lipids by classes and subclasses [20–24].

Trapped ion mobility spectrometry (TIMS) has been introduced relatively recently as an advantageous alternative technology to conventional IMS techniques [25–27]. In TIMS the ions are held stationary in an applied electric field, while the drift gas flows along the TIMS analyzer axis, towards the entrance of the drift tube. Instead of a stationary buffer gas as in conventional drift-time ion mobility (DTIM) or traveling-wave ion mobility (TWIM), TIMS uses a high flow of buffer gas that causes larger changes in ion trajectories by additional ion-neutral collision and "trapping" ions in the neutral gas phase according to their mobilities. The trapping and ejection of the ions in the drift tube are controlled by the electrical field that may be adjusted according to application requirements, resulting in higher resolution and significant flexibility of this technique. Unlike for other IMS systems, the resolution power in TIMS does not have a theoretical limit, as it is not restricted by the geometric length of the device [25,28]. Furthermore, TIMS benefits from a relatively simple calibration for determination of reduced mobility or collision-cross-section values, using internal or external standards for each set of experimental conditions. Overall, this technique excels in the separation of common interferences, providing higher throughput analysis, increased voltage-scan rate and peak capacity and reduction of the chemical noise.

Spectacular separations of isomers and analytes with small differences in mass/mobility were achieved using TIMS, obtaining up to eight times higher resolution of peptides with respect to conventional IMS techniques [29,30]. Also, high-resolution separations of isomeric environmental metabolites [31], polyaromatic hydrocarbons [32,33], carotenoids [34] and proteins [35–37] were achieved. A considerable number of studies have been dedicated to separation of "tuning-mix" calibration standards [25,27,28,38,39] focused on fundamental understanding of this reasonably new technique. However, the number of applications of TIMS to complex biological samples is limited to date [40,41].

Another example of a multidimensional approach that provides an increased separation power in the analysis of highly complex mixtures is comprehensive two-dimensional liquid chromatography (LC × LC). In LC × LC the combination of different column selectivities enables the separation of the components of lipid mixtures according to their chemical structures. One of the main requirements in developing a successful LC × LC method is to exploit two separation mechanisms that are as different as possible. This is reflected in a high occupation of the entire separation space.

Lipid extracts consist of components with a great variety of polarities (covering non-polar and polar classes) with a considerable molecular diversity within a given class. Reversed-phase liquid chromatography (RPLC) (*e.g.* using octyl, C8, or octadecyl, C18, types of stationary phases) offers a high selectivity in differentiating the degree of hydrophobicity of fatty acids alkyl chains. It has been successfully used in a large number of non-targeted lipid analyses [42–44] and it has been the method of choice in more than 70% of all publications on LC–MS-based lipidomic analysis [45]. Another LC separation mode used to characterize lipids is normal-phase LC (NPLC) [4,46–50]. In this technique the selectivity is such as to distinguish lipids according to the different polarities of their head groups. Because of the amphiphilic nature of the molecules, RPLC × NPLC is an obvious combination to consider. However, significant solvent-immiscibility issues arise when trying to realize on-line coupling of RPLC and NPLC with state-of-the-art (loop-type) LC × LC interfaces [51]. Such issues may possibly be overcome by evaporation of the solvents in off-line LC × LC [52]. Online coupling may be realized using solvent evaporation [53,54], by changing the sample solvent based on thermal effects [55] or by using adsorptive traps [56]. However, on-line RPLC × NPLC coupling tends to require sophisticatedly engineered interfaces.

Hydrophilic-interaction liquid chromatography (HILIC) is an increasingly popular alternative to NPLC. It features similar selectivity [46], but does not have significant solvent-compatibility issues when combined with RPLC, because HILIC employs aqueous-organic mobile phases containing considerable amounts of water. Moreover, HILIC tends to show a better repeatability, shorter equilibration times and longer column life times than traditional NPLC, due to the presence of buffers, which prevent column degradation [7,57,58]. RPLC and HILIC form an increasingly common combination that provides high selectivity and reasonable mobile-phase compatibility. Hence, this combination was chosen for our study. Combinations with HILIC in the first dimension (HILIC × RPLC) are commonly used, either in off-line or stop-flow modes [52,59–62]. Off-line approaches allow optimization of both dimensions almost independently, and, thus, provide maximum performance, without the time-limitations encountered in the comprehensive on-line approach. However, off-line result in long analysis times and are more difficult to automate. Using RPLC in the first dimension may be more advantageous for on-line coupling, as there are many more variations in the non-polar fatty-acid moieties of lipids that determine hydrophobic interaction in RPLC compared to the polar head-group structures. The first-dimension separation allows a longer run time and, thus, provides more separation power. Because of the lower number of classes and large differences in polarity between the lipid classes, separation in HILIC can be achieved faster and on shorter columns [7,63]. Therefore, in our study reversed phase was used in the first-dimension and HILIC in the second dimension.

The goal of our work was to develop a three-dimensional untargeted LC × LC–MS (coupling RPLC with HILIC) and LC-TIMS–MS methods, utilizing a prototype of this type of ion mobility instrument (TIMS), covering the separation of the major lipid classes in a complex human-plasma sample. To the best of our knowledge, TIMS has not yet been applied for lipidomic analysis. Fundamental aspects of the main factors influencing TIMS resolution for lipids have been investigated.

We aimed to evaluate both techniques in practice from a comprehensive untargeted lipidomics-profiling perspective. The

strengths and weaknesses of these two different analytical strategies are discussed.

## 2. Experimental

### 2.1. Reagents and materials

Acetonitrile (ACN), methanol, formic acid and 2-propanol (IPA), methyl-*tert*-butyl-ether (MTBE), all LC–MS grade, were purchased from Sigma-Aldrich (Steinheim, Germany). Water, LiChrosolv grade, was obtained from Merck (Darmstadt, Germany). Ammonium formate, 99% crystalline, was from Alfa Aesar (Karlsruhe, Germany). Pooled human plasma was purchased from Biowest (Nuaillé, France).

### 2.2. Lipid standards

For preliminary optimization of separations a mix of ten commonly targeted synthetic and natural extracted lipid standards was used (Differential Ion Mobility System Suitability LipidoMIX; see Table 1). A stock solution of 100 mg/L was prepared in chloroform-methanol (2:1, v/v) and stored at −20 °C. The working standard solution (10 mg/L) was obtained by evaporation of initial solvent and dilution in IPA-ACN-water (4:3:1, v/v/v). For the final multidimensional separation human plasma samples (90 μL) were spiked with 10 μL of a deuterium-labelled lipids mixture (SPLASH LipidoMIX Mass Spec standards) containing the major lipid classes in different concentrations (see Table S1 in Supplementary). Both mixtures were purchased from Avanti Polar Lipids (Alabaster, AL, USA).

### 2.3. Sample preparation

A modified Folch method [64] with MTBE/MeOH was used for the lipid extraction from human plasma [65]. Briefly, 300 μL of MeOH were added to 20 μL of the plasma and after short vortexing the solution was held at room temperature for about 10 min. Then, 1000 μL of MTBE were added and vortexed for 10 min. Next, 270 μL of water were added and the mixture was vortexed for another 10 min. After the mixture was centrifuged for 10 min at 13,000 rpm, the collected upper organic-phase layer was dried in a vacuum centrifuge evaporator. Extracted lipids were dissolved in 200 μL of IPA-ACN-water (4/3/1, v/v/v) for further analysis.

### 2.4. Instrumentations and methods

#### 2.4.1. LC × LC–MS analysis

LC × LC–MS experiments were carried out on an Agilent 1290 Infinity system (Agilent Technologies, Waldbronn, Germany), consisting of an Agilent 1100 HPLC binary pump (G1312A) for the first dimension and an Agilent Infinity 1290 UPLC binary pump (G4220A) for the second, a thermostatted column compartment (G1316C) with 2-position/6-port ultra-high pressure valve head (1200 bar) and a Valve Drive (G1170A) with 2-position/4-port-duo valve (2D-LC Valve Head, 1200 bar) equipped with two identical 20-μL sampling loops. Agilent modules were controlled using Agilent Chemstation C.01.07 software.

For the first-dimension separation an Acquity UPLC ethylene-bridged hybrid (BEH) C18 column (150 × 2.1 mm i.d., 1.7-μm particles; Waters, Milford, MA, USA) was used under the following conditions: flow rate 20 μL/min; injection volume ($V_{inj}$) 10 μL of human plasma or 1 μL of standard mixture, respectively. Separations were performed at a temperature of 65 °C. Mobile phase A was ACN/$H_2O$ (60/40, *v*/*v*) and mobile phase B was IPA/ACN (90:10, *v*/*v*). Both A and B contained 10 mM ammonium formate. The separation was performed using the following gradient program: 40% B at 0 min, 0–167 min, 40–99%B, 167–168 min 99%B, in 0.1 min returned to initial conditions and kept constant (168.1–190 min) for column re-equilibration. The total analysis time was 190 min.

For the second dimension separation an Acquity BEH UPLC HILIC column (50 × 2.1 mm i.d., 1.7-μm particles; Waters) was used under the following conditions: flow rate 2 mL/min; column temperature 40 °C. Mobile phase A was an aqueous solution of 10 mM ammonium formate and mobile phase B was acetonitrile. The separation was performed using the following gradient program: 95%B at 0 min; 0–0.01 min, from 95% to 90%B; 0.01–0.8 min 80%B and 0.81–1 min, 95%B (re-equilibration). The post-column flow was reduced through a T-piece union with splitting ratio of 1:3 prior to detection. The modulation time was 60 s.

MS detection was performed on an Agilent 6540 Ultra-High-Definition Accurate-Mass Quadrupole Time-of-Flight (Q-TOF) mass spectrometer equipped with a Jetstream Electro Spray Ionization source (Agilent Technologies, Santa Clara, CA, USA). Measurements were carried out in the positive ionization mode with a scan range of *m*/*z* 50–1000 and a scan frequency of 6 Hz. The capillary voltage was set at 3500 V, nebulizer gas (nitrogen) at 35 psi (2.4 bar), with a sheath-gas flow rate of 7.5 L/min at 350 °C and a drying gas flow rate of 10 L/min at 300 °C. The Q-TOF was calibrated on a daily basis using the ESI Tuning mix mass spectrometry standard (Tunemix, G2421A; Agilent).

#### 2.4.2. LC-TIMS-MS analysis

LC-TIMS–MS experiments were performed on a Dionex Ultimate 3000 ultra-high performance liquid chromatography system (ThermoFischer Scientific, Germering, Germany) coupled to a prototype ESI-TIMS-QTOF mass spectrometer (Bruker Daltonics, Bremen, Germany).

In order to have comparable LC analysis for both methods, the RP separation was carried out using the same separation conditions, described above for the first dimension in the LC × LC approach.

After LC separation the sample was introduced into an orthogonal ESI source (Bruker Daltonics) operated in positive ionization mode with a scan range of *m*/*z* 50–1000. The capillary voltage was 4700 V with end-plate offset −500 V. Nitrogen was used as a nebulizer gas at 0.5 bar. The drying gas was set to 4.0 L/min at a temperature of 180 °C. The acquisition rate was 6 Hz.

Detailed information about the TIMS instrument can be found in the literature [25,26,28,35]. TIMS separation was performed using nitrogen as a bath gas at 300 K, the gas flow velocity was controlled by the difference between pressure at the entrance ($P_1$) and the exit ($P_2$) of the funnel. A difference ($P_1 - P_2$) of 1.9 mbar was used for all experiments. Operational parameters of the TIMS cell were investigated in the current study and were finally set as follows: voltage ramp $\Delta V$ = 130 V for the analysis with a wide range of mobilities; ramp time (separation time) 120 ms; RF amplitude 250 Vpp; accumulation time of a single analysis 20 ms, acquiring 1400 ToF pulses per IMS scan. All data were summed across 380 analysis cycles, *i.e.* 30.3 s per cycle. Operation was controlled using two different computers. The first computer was used to control the LC system using Chromeleon 6.80 software (ThermoFischer) and the QTOF instrument using Compass 1.3 software (Bruker Daltonics), while the second computer controlled the TIMS tunnel *via* TIMS Data Viewer 1.4.0.27015 (Bruker Daltonics) and acquired the data. The Tuning Mix MS standards (Tunemix, G2421A, Agilent Technologies, Santa Clara, CA, USA) was used for mass and mobility calibration. Determination of reduced-mobility ($K_0$) and collision-cross-section (CCS) values was based on calibration standards with known mobilities (*m*/*z* 622, $K_0$ = 1.013 $cm^2\ V^{-1}\ s^{-1}$ and *m*/*z* 922, $K_0$ = 0.835 $cm^2\ V^{-1}\ s^{-1}$) [27]. The TIMS mobility calibration procedure and the methods of calculation can be found elsewhere [25,27,29,35].

**Table 1**
List of lipids standards, their detection details and $K_0$ and CCS values (see explanation below), used for optimization purposes in this study.

| Lipid class | Abbreviation | Lipid species level[a] | *m/z* | Adduct | Reduced mobility $K_0$ ($cm^2\ V^{-1}\ s^{-1}$) | CCS ($Å^2$) | CCS (ref) ($Å^2$) |
|---|---|---|---|---|---|---|---|
| Lysophosphatidylcholine | LPC | (18:1) | 522.36 | $[M+H]^+$ | 0.879 | 231.8 | 230.8[b] 240[c] 236.2[d] |
| Diacylglycerol | DG | (14:1/14:1) | 526.44 | $[M+NH4]^+$ | 0.864 | 235.3 | – |
| Phosphatidylethanolamine | PE | (14:1/14:1) | 632.43 | $[M+H]^+$ | 0.801 | 249.6 | – |
| Ceramide | CER | (18:1/18:1) | 564.53 | $[M+H]^+$ | 0.776 | 255.4 | 257.6[b] |
| Phosphatidylserines | PS | (14:1/14:1) | 676.42 | $[M+H]^+$ | 0.763 | 258.2 | – |
| Phosphatidylcholine | PC | (14:1/14:1) | 674.48 | $[M+H]^+$ | 0.730 | 265.8 | – |
| Phosphatidylglycerol | PG | (14:1/14:1) | 680.45 | $[M+NH4]^+$ | 0.669 | 279.8 | – |
| Sphingomyeline | SM | (18:1/18:1) | 729.59 | $[M+H]^+$ | 0.632 | 288.2 | 283.2[b] |
| Phosphatidylinositol | PI | (14:1/14:1) | 751.44 | $[M+H]^+$ | 0.631 | 288.4 | – |
| Triacylglycerol | TG | (18:1/18:1/18:1) | 902.82 | $[M+NH4]^+$ | 0.463 | 326.6 | – |

[a] The lipid notation follows the recommended shorthand nomenclature according to [75].
[b] Ref. [76].
[c] Ref. [22].
[d] Ref. [18].

TIMS resolution was calculated from

$$R = \frac{K}{\Delta K} = \frac{V_{out} - V_{elut}}{\Delta V} \quad (1)$$

where $V_{elut}$ is the elution voltage of the ion, which is a characteristic parameter for the mobility with a given same bath gas and velocity, and $V_{out}$ is the voltage applied to the last electrode. $\Delta V$ is the width of the peak at half height.

### 2.5. Data processing

LC × LC–MS data analysis and visualization were performed using GC Image R 2.5 software (GCimage, Lincoln, NE, USA). LC-TIMS–MS separations were interpreted by Compass DataAnalysis 5.0 software (Bruker Daltonics). For the feature extraction all raw data were converted to .mzXML files and exported into open-source MZmine 2 data processing software [66,67]. Mass detection, chromatogram builder, deconvolution isotopic grouper with following peak row filter, and RANSAC peak alignment were set with *m/z* tolerance of 0.005, retention time tolerance of 0.05 min and *m/z* range of 260–1000. Ion-adducts search and generation of the list of precursor ions were accomplished using the online MS-analysis tool ("General MS precursor ion search on multiple lipid classes") using the online Lipid Maps database based on accurate *m/z* values (with 0.001 *m/z* tolerance) of lipidomic features [68]. Preliminary identification of the lipid species was performed manually by matching first-dimension retention times and *m/z* values with the second-dimension retention times for LC × LC–MS data and mobility scan values for LC-TIMS–MS data, respectively.

## 3. Results and discussion

### 3.1. RPLC × HILIC–MS separation

In RPLC, mobile phases (usually containing mixtures of water with organic solvents, such as ACN or MeOH) typically with addition of a strong solvent (*e.g.* 2-propanol or THF) and elevated temperatures (*e.g.* 65°–80 °C) are used to ensure elution of the strongly retained lipids (TG and CE) from the column and to shorten the analysis time [42,69–71]. The RPLC method development in the current study was based on the optimal conditions reported in [69,72] and modified as described above in Experimental. As modifier 10 mM ammonium formate was used, since it was found to yield higher signal intensities for the formed $[M+NH4]^+$ adducts compared to $[M+H]^+$ adducts for some lipid classes in positive ionization mode (ESI(+)) [73].

A solution of ten pre-mixed synthetic lipid standards combined with natural lipids extracts was prepared to contain one representative of each lipid class. This mixture was used for the preliminarily optimization of the individual 1D separations (for abbreviations and details see Table 1 below). Representative ions of the lipids classes SM, LPC, PC, PS, PE, PI and CER were mainly detected as protonated $[M+H]^+$ ions, while PG, TG and DG were observed with higher abundance as ammonium adducts $[M+NH_4]^+$ with traces of $[M+Na]^+$ in positive ionization mode.

The overlaid extracted-ion chromatograms of the RP-(ESI+)-MS analysis of the mixture of lipid standards are shown in Fig. 1a and the total-ion-current chromatogram of a lipids extract of human plasma separated under the same conditions is shown in Fig. 1b.

As can be seen from the chromatogram (Fig. 1a) the mixture of lipid species showed a broad range of retention times, spanning the entire chromatogram. Retention increased in order of increasing hydrophobicity of the compounds and the elution order was in agreement with the literature [42,72,74]. Because the PS, PG, PE and PI lipid classes are typically better ionized in the negative ionization mode, relatively low intensities were observed in the present experiment. The separation of human plasma (Fig. 1b), analysed under the same conditions, demonstrates a clear example of the sample complexity.

During the development of the second dimension separation the peak capacity was investigated as a function of the gradient time ($t_g/t_0$) and the linear velocity (υ, mm/s) (Fig. S1a and S1b in Supplementary Material). The experimental study showed an approximate square-root dependence of the peak capacity on the gradient time, whereas increasing the flow rate only led to a minor decrease in peak capacity.

In on-line LC × LC, the second dimension separation time is critically important. The total analysis time of the second dimension (including the gradient and the necessary re-equilibration time) is equal to the sampling time of fractions from the first-dimension effluent. As shown in Fig. S1b, longer gradients result in greater separation power. The second-dimension ($^2$D) separation is supposed to be fast to ensure sufficient sampling of the peaks eluting from the first dimension (typically 2–3 cuts per peak), while it should also provide a good deal of separation power (peak capacity). It must be kept in mind that faster gradients lead to poorer resolution and that insufficient equilibration time may impact the quality and repeatability of the separation. Therefore, a compromise should be struck between the duration of the gradient, the equilibration time and the total sampling time.

Our optimization resulted in a $^2$D separation with a cycle time of 1 min when operating at a flow rate of 2 mL/min. In contrast

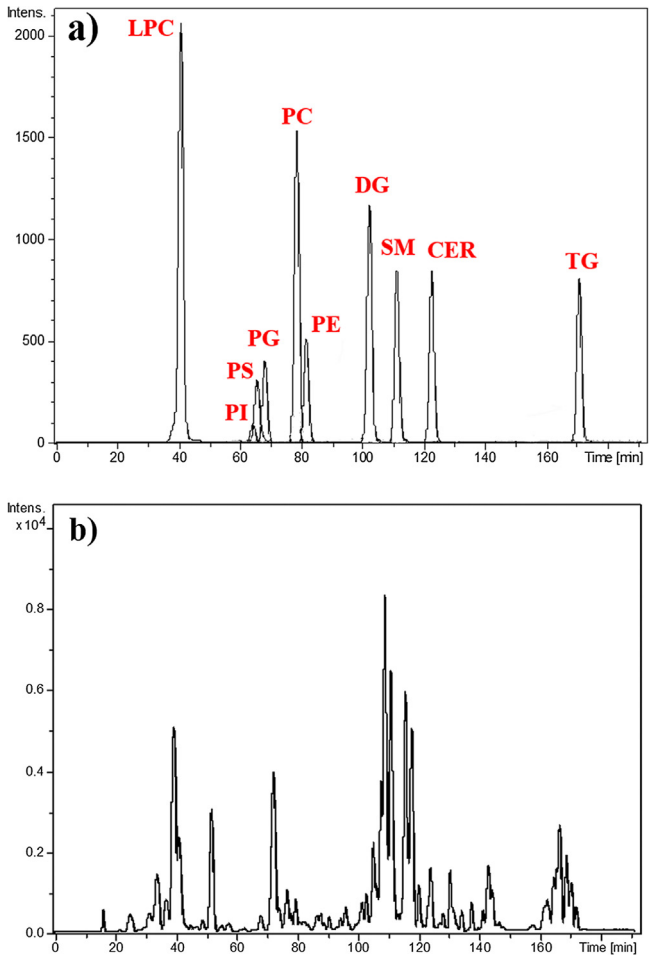


**Fig. 1.** RP-ESI–MS analysis of a: mixture of lipid standards (overlaid extracted-ion chromatograms); and b: lipids extract of human plasma (total ion chromatogram), detected in positive ionization mode. The separation conditions are reported in Experimental. Standards are: Lysophosphatidylcholine (**LPC**), Phosphatidylinositol (**PI**), Phosphatidylserine (**PS**), Phosphatidylglycerol (**PG**), Phosphatidylcholine (**PC**), Phosphatidylethanolamine (**PE**), Diacylglycerol (**DG**), Sphingomyeline (**SM**), Ceramide (**CER**), Triacylglycerol (**TG**). (For analyte identification and selected ions see also Table 1 below).

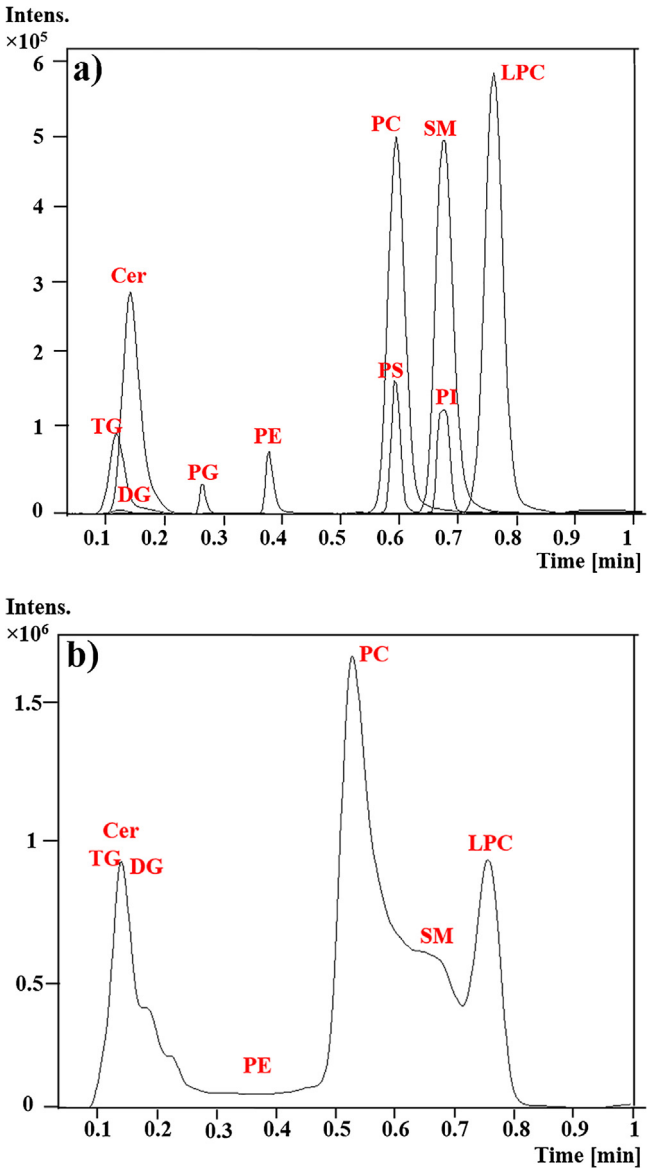


**Fig. 2.** Class separation of lipids by HILIC-ESI–MS, detected in positive ionization mode. a: mixture of lipids standards (overlaid extracted-ion chromatograms); b: lipids extract of human plasma (total-ion chromatogram). For separation conditions see Experimental. For analytes' abbreviations and identification see Table 1.

with RPLC, HILIC provides a separation by classes of polar head groups, with the more polar classes being more retained. As shown in the chromatogram of Fig. 2a compounds that belong to non-polar lipid classes (*i.e.* DG, TG and CER) elute first, close to the column dead volume ($t_0$), while more polar classes (PE, PC, PS, SM, LPC *etc.*) are resolved according to their polarity. Holčapek et al. [63], recently reported short lifetimes of the fully porous $^2$D columns. We no longer observed such issues using our optimized method. We achieved an efficient separation of lipid standards with a higher peak capacity ($^2n_c = 8$ *vs.* $^2n_c = 4.5$ in Ref. [63]). By using narrower $^2$D columns (2.1 mm i.d.), employing lower $^2$D flow rates, and decreasing the split ratio prior MS, the sensitivity of the method was significantly enhanced.

As can be seen in the chromatogram resulting from the separation of the human plasma (Fig. 2b), fast HILIC gradients on short columns (50 mm) do not provide high-resolution separations of the sample within the one-minute time frame. However, it provides a class-type characterization of the lipids (Fig. 2a) offering additional selectivity that is essentially complementary to RPLC for comprehensive two-dimensional liquid chromatography (LC × LC) analysis.

The optimized on-line RP × HILIC-MS analysis was applied for the separation of a lipids extract of human plasma (Fig. 3). In untargeted lipidomic studies internal standards are commonly used to enhance the robustness (*i.e.* mass accuracy and retention-time precision) of the analysis and to estimate the recovery [77,78]. A cocktail of deuterated lipids was added to the human plasma extract to obtain additional information for initial classification of molecular species (see Table S1 in Supplementary Material).

Because of the extremely large variations in concentrations of the various lipid species present in the plasma sample and because of background interferences, the raw LC × LC chromatograms do not provide a good illustration of the actual separation. Several data-treatment steps had to be performed before an acceptable visualization was attained. The most intense peaks in the spectra (roughly 150 components) belonging to each lipid class from the obtained total-ion chromatograms were selected and the associated $m/z$ values were imported in the GC Image software to obtain extracted-ion chromatograms (EICs) from the TIC. The summation of all EICs is shown in Fig. 3.

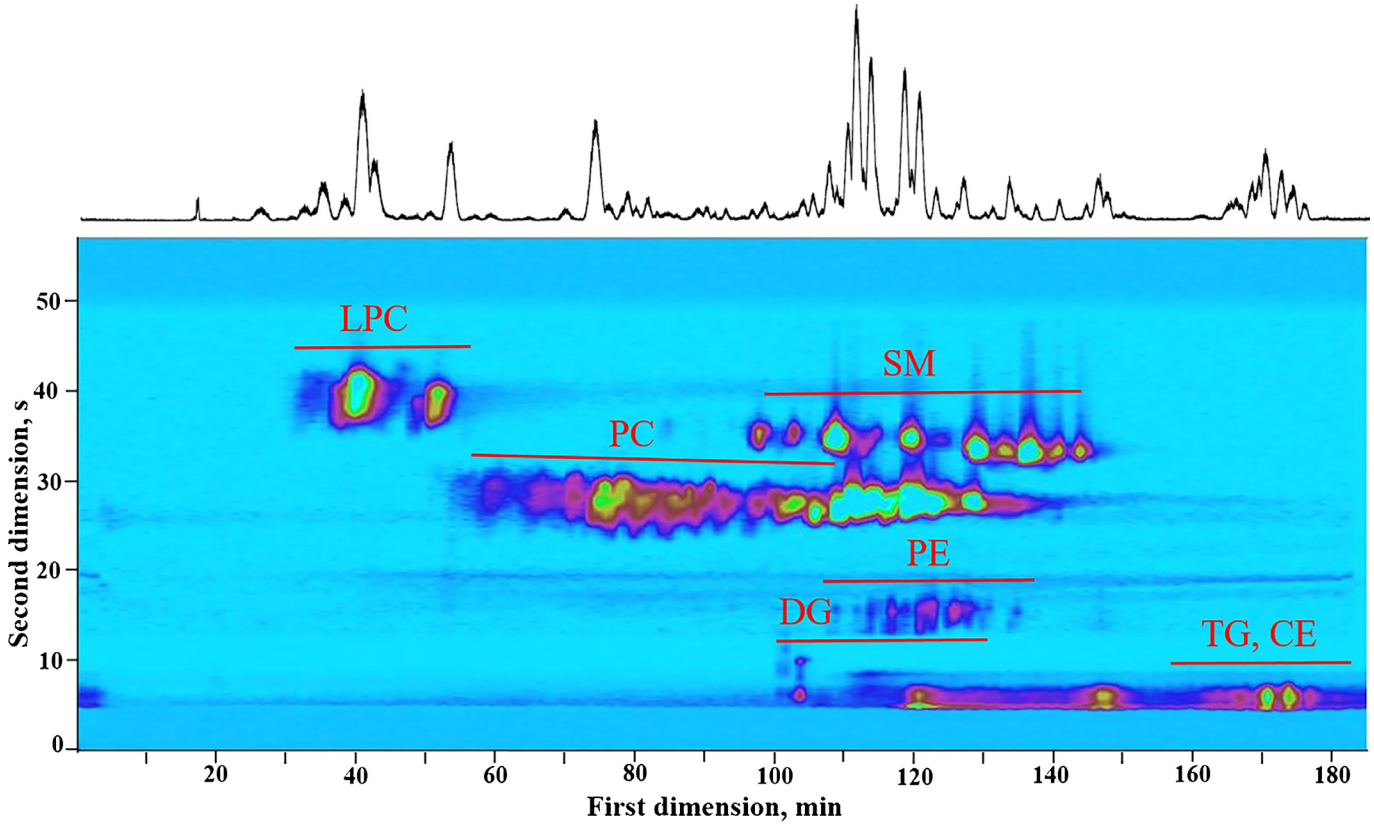


**Fig. 3.** Reconstructed LC × LC chromatogram (sum of extracted-ion chromatograms) of lipids extract from human plasma separated by RP × HILIC-ESI (+)-MS under optimized conditions. Tentative regions in the LC × LC chromatogram are assigned to different classes of lipids based on retention times of tentatively identified molecular features in conjunction with retention times of internal standards added to the sample. Chromatographic and detection conditions are provided in the Experimental section.

The preliminary identification was performed based on matching the measured accurate *m*/*z* values with the publicly available online Database of Lipid Maps (LMSD) [68], in combination with the retention times in the first and second dimensions, and supported by retention times of the isotope labelled lipid standards added to the plasma sample (Table S1, Supplementary Material). In total, about 100 lipid species, belonging to the major lipid classes were tentatively assigned (see Table S2, Supplementary Material).

### 3.2. LC-TIMS–MS separation

A main advantage of TIMS is the large number of parameters that can be selected and optimized by the user for a specific application and analytical purpose. According to TIMS theory, the bath-gas velocity, electric-field ramp speed and RF amplitude are the main parameters to control resolution and overall separation performance [25]. The electric-field range, applied on the tunnel of the instrument, defines the mobility range of the trapped ions. At a constant bath-gas velocity, the resolution is directly related to the electric-field ramp speed – ($\Delta V_{ramp}/t_{ramp}$), *i.e.* the variation in differential potential across the tunnel with time. A lower ramp speed yields a higher resolution. The voltage range should be set in accordance with the objective of the analysis. For a high resolution, for example for the separation of geometric isomers, a narrow voltage range is preferred ("high-resolution separation"). In case when general information on the sample is needed across a relatively wide range of ion mobilities, a broad voltage range will be more appropriate ("low-resolution separation"). Hence, to accomplish the comprehensive non-targeted analysis of human plasma, parameters were optimized around a broad voltage gradient, so as to separate multiple lipid classes in one multidimensional run. All experiments for parameter optimization were performed in a so-called "shotgun" manner, directly infusing the diluted mixture of lipids standards at 20 μL/min flow rate into the TIMS-MS instrument.

First, the strength of the electric field-gradient (EFG or $\Delta V_{ramp}$) was varied, *i.e.* the potentials at the start and the end of the TIMS analyser section at a constant ramp time of 45 ms. The effect of the EFG on the position and resolution of lipid standards at various points in the mobilograms is depicted in Fig. 4 (a–e; voltages indicated for each case by numbers in grey colour). Decreasing $\Delta V_{ramp}$ from 250 to 80 and, consequently, the ramp speed (indicated in the figure) led to an observable gain in resolution and a good coverage of the separation space at a ramp speed of 2.9 V/ms (Fig. 4, case d). A high starting value (*e.g.* −150 V, Fig. 4e) prevented the bigger ions from being trapped and led to a "wrap-around" effect.

After the range of the EFG was defined, its duration ($t_{ramp}$) was studied. Fig. S2 shows the variation of resolution as a function of ramp time for a mixture of lipid standards. As an example, four lipid standards belonging to different lipid classes with a reasonable difference in molecular weights are shown. Similarly to a previous investigation [26], an increase in ramp time led to an increase in resolution.

The RF amplitude (Vpp) plays an important role as a radial force that confines ions and prevents diffusion between the walls of the TIMS analyser. Fig. S3 shows an example of the variation of signal intensities with increasing RF amplitude. An RF amplitude of 250 was found to be sufficient for all lipid classes.

The optimized experimental parameters discussed above were next tested by coupling TIMS with RPLC as a first separation dimension. A spectrum of ion intensity plotted against mobility (or scan number in our case) is typically called a "mobilogram". An exam-

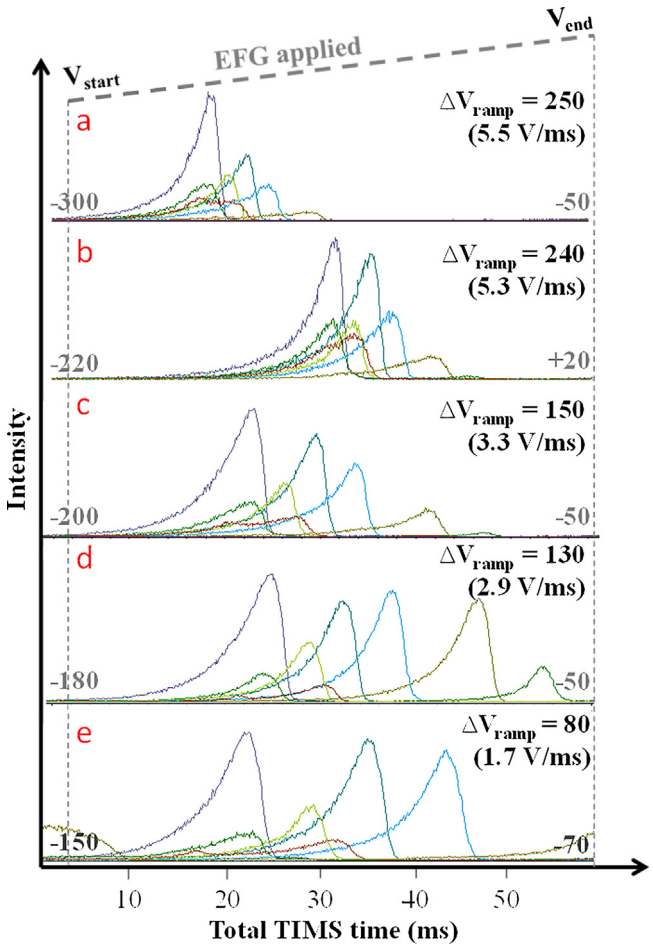


**Fig. 4.** Schematic illustration of the effects of the electric field gradient and the starting and ending voltages (cases a-e) of the TIMS tunnel on separation of lipid standards. $t_{ramp}$ was kept constant (45 ms).

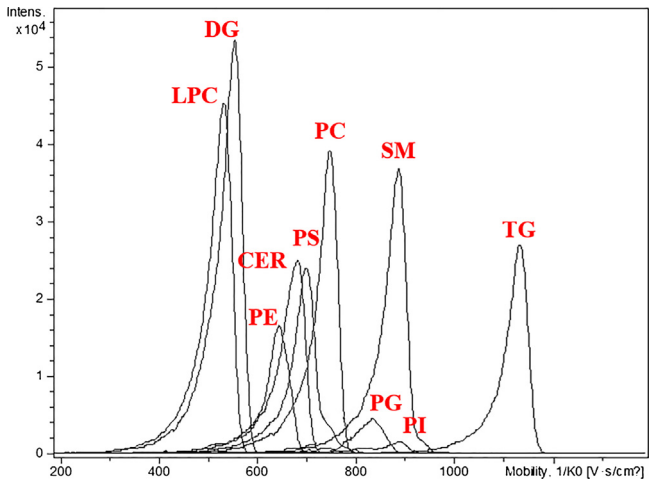


**Fig. 5.** Extracted-ion mobilogram for the mixture of lipid standards separated by LC-TIMS–MS under the optimized conditions. For analytes' identification and selected ions see also Table 1.

ple is shown in Fig. 5. TIMS separation of the mixture of ten lipid standards was achieved. The analysis of the major lipid classes presented here encompasses an additional challenge in comparison with previously reported analyses of the tuning standards or biomolecules, in which a higher TIMS resolution was obtained [27,33]. This can be explained by, first, by the shallow electric field gradient applied, covering a broad range of voltages, but *a priori* sacrificing resolution. Secondly, the molecules of these compounds, with their long alkyl chains, are bulky, causing them to rotate indefinably in the applied electric field. They hardly form compact structures in the gas phase and, therefore, give relatively broad tailing peaks, which contribute to the lower resolution. A similar tendency has been investigated by May et al., who reported that lipids exhibit the largest CCS values among a range of biomolecules, because of the their inability to form packed, self-solvated structures in the gas-phase [21]. Additionally, according to TIMS theory [25], resolving power is linearly dependent on the bath-gas velocity. It can be controlled by varying the pressure differences at the entrance ($P_1$) and the exit ($P_2$) of the TIMS analyser. Furthermore, reducing the bath-gas temperature will cause the ion diffusion to decrease and the resolution to increase. Therefore, by increasing the velocity of the gas and decreasing the temperature the TIMS separation performance may be further improved. However, in the current pre-commercial research instrument we were not able to manipulate bath-gas parameters.

It is impossible to determine CCS values from the obtained mobilograms using straightforward calculations. Therefore, analogous to the situation in TWIM, a calibration has to be performed for data interpretation. The measured mobilities of the standards were converted to the reduced mobility values ($K_0$) and collision cross sections (CCS) shown in Table 1. Reduced mobility, *i.e.* ion mobility normalized for temperature and pressure, is a standard means to report IMS results. The external calibration performed in this study is described in Experimental. Calculated values reported in Table 1 are in agreement with the values obtained in previous studies reported in the literature [18,79,80] for the same lipid species, indicating that the choice of the calibrant may not have as significant impact on CCS values observed with TIMS as it does for the TWIMS-MS platform [81,82]. The ability to use non-specific and non-lipid calibrants is a considerable advantage of the TIMS-MS technique, as it provides the opportunity to rapidly build a comprehensive database of CCS values for large datasets in untargeted lipidomics analysis. However, a systematic evaluation of the accuracy of the obtained CCS values was not within the scope of the present study.

Incorporation of a TIMS stage between LC and MS resulted in the LC-TIMS–MS heat map shown in Fig. 6. The data were plotted as a 2D graph with mobility scan values *versus* LC (first-dimension) retention time in order to demonstrate the achieved separation performance of both dimensions. This clearly demonstrates a highly informative structural separation of the complex sample, revealing a great number of compounds with equal retention times, but separated in the ion-mobility dimension. The analysis of LC-TIMS–MS data revealed approximately 800 molecular features. The tentative assignment of individual lipid classes was based on direct correlation of the LC, IMS and MS data of the isotopically labelled internal lipid standards belonging to ten lipid classes spiked with the plasma. We limited ourselves to estimating the region of elution of certain lipid classes and counting the features presents, aiming to qualitative assess the separation power of the LC-TIMS–MS technique. In future work, such data, in combination with CCS databases should allow identification of more lipids with a good deal of certainty. The detection information, calculated reduced mobility, and collision-cross-section values for the labelled internal standards added to human plasma samples for LC-TIMS–MS measurements are listed in Table S1. Lipid species belonging to seven major lipid classes are listed in Table S2. For both methods species were tentatively identified with reasonable confidence. A much-more-thorough identification would additionally require MS/MS experiments for structural confirmation.

In fairness, similar results can be achieved within shorter analysis time (typically less than 30 min [11]) by utilizing UPLC sep-

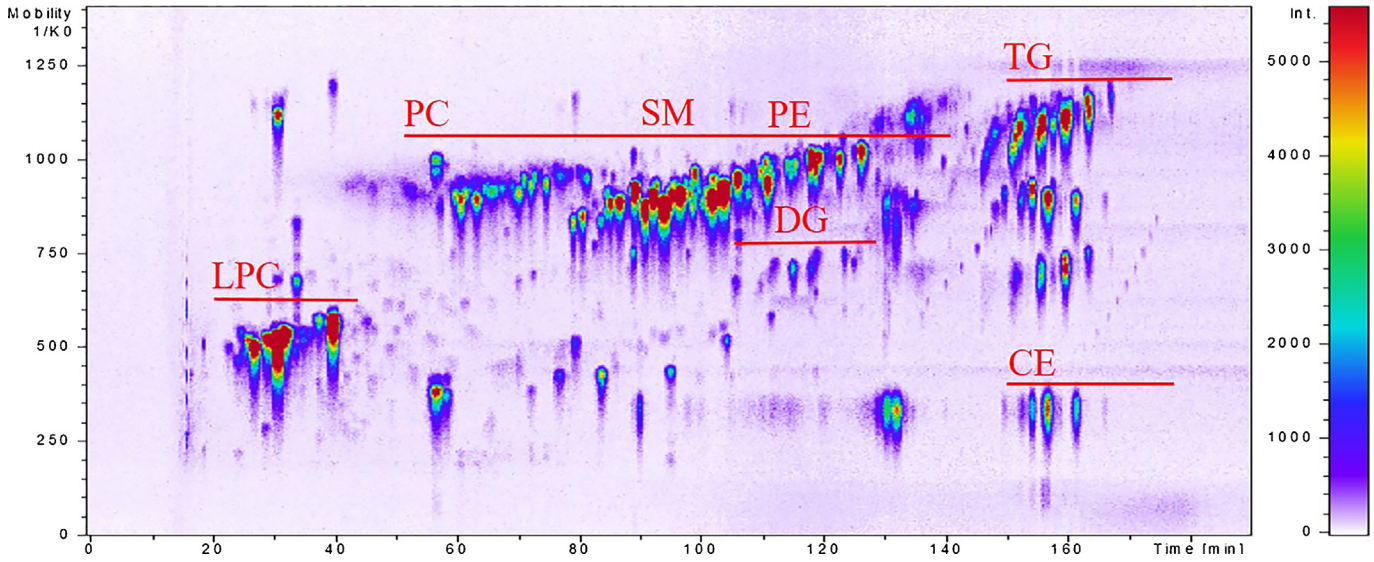


**Fig. 6.** LC-TIMS–MS separation of human plasma under optimized conditions acquired in positive ionization mode. Tentative regions are assigned to different classes of lipids (abbreviations as in Table S2).

aration technology. Beccaria et al. succeeded in identifying more than 100 lipids within 20 min using a UPLC–MS platform [83] and more than 280 species were discovered by Castro-Perez et al. with a run-to-run time of 15 min [84]. Ion-mobility-based separation approaches offer even faster analysis with high separation performance due to its fast duty cycle. About 200 lipids or/and their isomers were determined in 10–20 min [12,16,76,80] in combination with LC or in milliseconds by direct-infusion IMS [85,86].

However, the aim of the current study was not to compete with the highest number of identified lipids, nor to develop the fastest analysis from the pure lipidomics perspective. We intended to compare the theoretical separation power of the two multidimensional separation techniques that are currently gaining popularity. Thus, in order to keep the first dimension chromatographic methods comparable, the RP separation was chosen such as to meet the requirements of a first-dimension separation for LC × LC, resulting in a rather long analysis time and sub-optimal LC separation conditions.

### 3.3. Comparison of multidimensional separations of human plasma

#### 3.3.1. Orthogonality

The term "multidimensional separations", whether it is multidimensional chromatography or hyphenation of different separation techniques, assumes that the components are subjected to two or more separation mechanisms. If there is a high correlation between the resulting retention times, the full potential of the system is not realized and it may be more effective to perform a fully optimized less complex separation (such as LC–MS). Therefore, orthogonality is one of the most crucial factors when performing *n*-dimensional separations.

Introducing a third dimension between LC and MS, we were interested to characterize the degree of orthogonality of this additional dimension relative to the other two. Visual inspection of the chromatograms obtained for human plasma (Figs. 3 and 6) showed a good coverage of the separation space within the confines of two separation dimensions (*e.g.* RPLC × HILIC and RPLC × TIMS). For clarity and simplicity, the complementarities between the first and second dimensions were visualized by plotting normalized retention times of the lipid standards in HILIC or normalized mobility values from TIMS (Fig. 7) as a function of retention times in the (first-dimension) RPLC separation. The degree of orthogonality was estimated using the asterisk approach [87], which indicates the spreading of peaks around the separation space and is expressed as a percentage in the plots for each case (where a completely orthogonal system corresponds to $A_0$ is 100%). The graphs illustrating the surface coverage of ten lipid standards provides a rough idea of the selectivity of the combined separation dimensions.

The RPLC × HILIC combination provides a separation based on physico-chemical properties of compounds, which relates, for example, to the fatty alkyl chain lengths and to the polar head groups (lipid classes). The main lipid classes (Fig. 7a) give rise to an asterisk value ($A_0$) of 44%. The analysis by ion mobility implies a differentiation based on more physical properties of molecules, *i.e.* a cross-sectional area, related to the molecular size and shape. A good degree of orthogonality was observed between RPLC and TIMS, indicating even higher $A_0$ (64%) than obtained with RPLC × HILIC (Fig. 7b). In order to study the separation mechanism of TIMS, its correlation with the HILIC dimension was also examined (Fig. 7c). The elution order of the lipid species showed no significant correlation between the two mechanisms. Exceptions were observed for diacylglycerol (DG, the smallest and one of the most-polar molecules in the present sample), which eluted first in both cases and the completely overlapping signals of SM and PI (because of the small difference in molecular weight and the similar polarity of these compounds). Nevertheless, the findings above illustrate that a good complementarity could be achieved by combining TIMS with either RPLC or HILIC.

The role of the MS dimension is crucial in both three-stage hyphenated systems. Therefore, a simplified approach to evaluate the orthogonality, as well as the peak capacity of MS was also considered in this study. The correlations of the second and a third dimensions (*i.e.* HILIC × MS and TIMS × MS) could be depicted by plotting retention-time values of the standards mixture (and mobility values obtained directly from the mobilogram) against their *m*/*z* values (Fig. 8). As described in the optimization section, HILIC provides limited selectivity between lipid classes. However, its separation mechanism has a high degree of orthogonality with respect to MS.

As the mobility of ions is related to their size and, to a large degree, to their mass, the ion-mobility separation is highly correlated to MS as can be clearly seen on Fig. 8b. Fig. S4 shows the 2D IMS-MS plot of a human plasma sample, demonstrating the strong

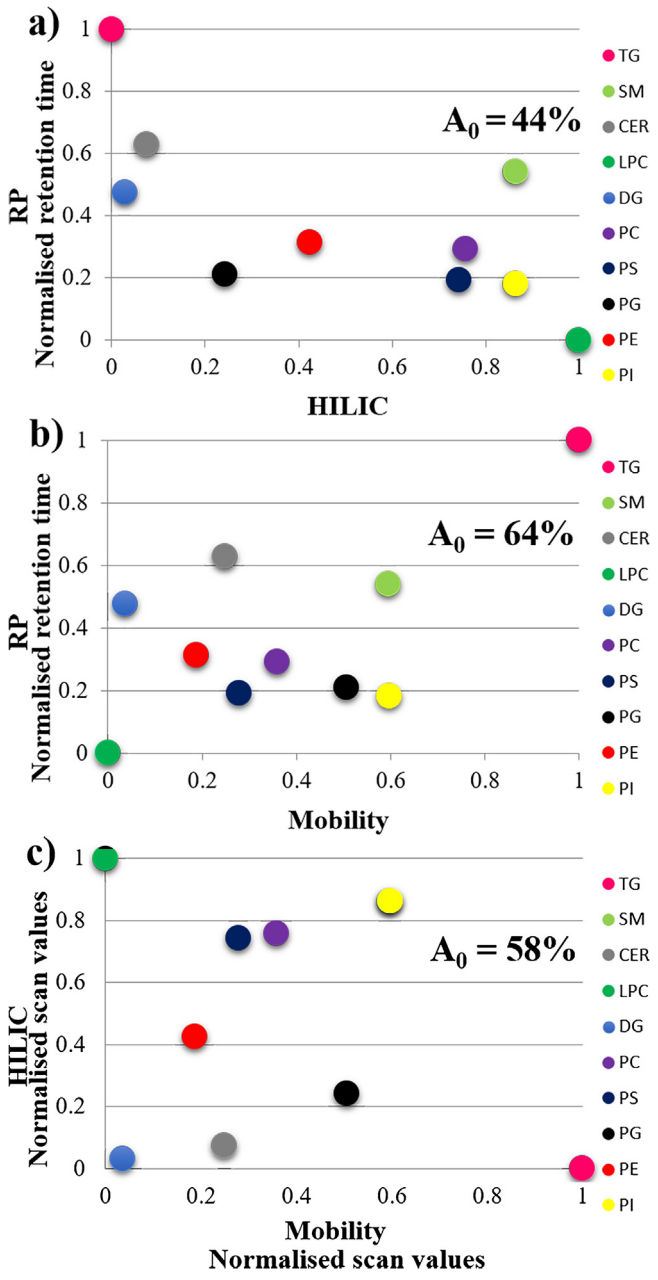


**Fig. 7.** Graphs illustrating the coverage of separation spaces by the lipid standards using RPLC × HILIC (a), RP × TIMS (b) and HILIC × TIMS (c). Normalized retention times or mobility values are plotted. The indicative degrees of orthogonality (asterisk values, $A_0$) are indicated on the graphs for each case.

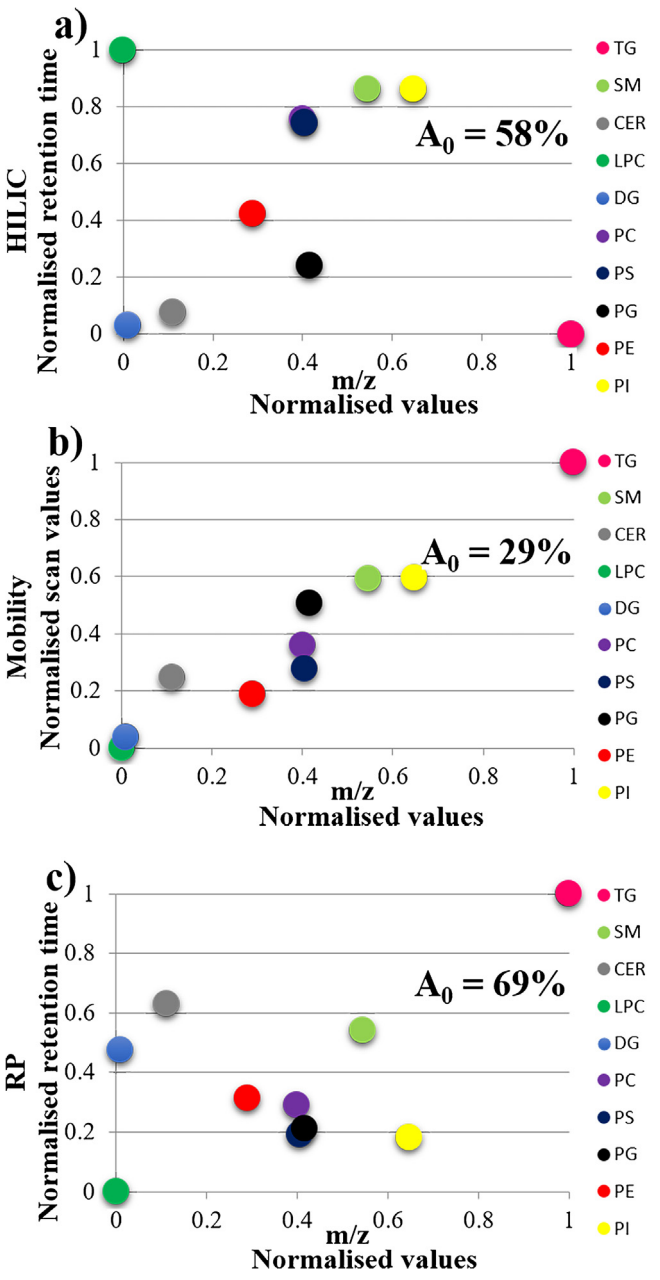


**Fig. 8.** Illustration of the correlation between MS and HILIC (a), TIMS (b), and RP (c) in the analysis of lipid standards. The tentative estimations of the degree of orthogonality (asterisk values, $A_0$) are indicated in the upper right corner for each graph.

mobility-mass-correlation and, consequently, poor orthogonality. This strong correlation may affect the overall separation power (see discussion in the next session) and it may complicate analyte identification. Thus, 100 lipid species were identified by LC × LC–MS analysis, but only about 55 by LC-TIMS–MS. The identity of the closely eluting compounds (*e.g.* lipids belonging to SM, PC and PE classes with similar *m*/*z* range and, therefore, mobilities) was more difficult to establish when relying the second (TIMS) separation dimension. Because of the orthogonality of RP and HILIC, the allocation of these classes using LC × LC–MS was more straightforward. The same tendency may be observed with LPE and LPC classes (see detection information for the deuterated lipid standards in Table S1).

### 3.3.2. Peak capacity and separability

Peak capacity is the theoretical number of peaks that may be separated with a given resolution under a given set of conditions. It is one of the most important parameters to evaluate separation power. The theoretical estimation of the peak capacity for combined LC-IMS–MS and LC × LC-IMS–MS approaches was recently described by Causon and Hann for non-targeted analysis strategies [88]. A theoretical maximum peak capacity of the order of $10^4$ was estimated for LC × IMS-MS. This peak capacity was shown to be comparable with experimental values for LC × LC–MS derived from literature data on metabolomics and proteomics applications. However, these estimates were based on the assumption of 100% usage of the separation space and they did not include practical limitations, such as undersampling, band broadening, dilution [89] and limited orthogonality.

The peak capacity ($n_c$) in gradient-elution LC can be calculated from:

$$n_c = 1 + \left(\frac{t_G}{w_{av}}\right) \quad (2)$$

where $t_G$ is a gradient time and $w_{av}$ represents an average peak width at the baseline. $w_{av}$ was estimated from the major peaks in the chromatogram of the human plasma sample. The theoretical peak capacity of a two-dimensional separation can be estimated from

$$n_c = n^{/>}c \times n^{/>}c \quad (3)$$

using the values obtained from the one-dimensional runs for the first ($n^{/>}c$) and second ($n^{/>}c$) dimensions, respectively.

This estimation is not taking into account the undersampling effect, occurring in practice due to the modulation process. This can be corrected for using the equation proposed by Li et al. [90]:

$$\mathrm{n_c} = \frac{\mathrm{n^{/>}c \times n^{/>}c}}{\beta} = \frac{\mathrm{n^{/>}c \times n^{/>}c}}{\sqrt{1 + 3.35 \times \left(\frac{\mathrm{t^{/>}cn^{/>}c}}{\mathrm{t^{/>}G}}\right)^2}} \quad (4)$$

where β is the under-sampling correction factor due to modulation, $t^{/>}c$ is the second-dimension cycle time and $t^{/>}G$ is the first-dimension gradient time [46].

In analogy with chromatography, the peak capacity of TIMS analysis can be expressed based on the full peak width in voltage units ($W \approx 1.7$ times the peak width at half maximum) across the applied voltage range ($\Delta V_{\mathrm{ramp}}$) [91]:

$$n_c = \frac{\Delta V_{\mathrm{ramp}}}{W_{\mathrm{av}}} = \frac{(V_{\mathrm{max}} - V_{\mathrm{min}})}{W_{\mathrm{av}}} \quad (5)$$

where $V_{\mathrm{max}}$ and $V_{\mathrm{min}}$ are the starting and ending potentials applied on the TIMS tunnel, and $W_{\mathrm{av}}$ is the average peak width observed in the mobilogram of the human plasma.

The gain in peak capacity associated with the "mass spectrometry dimension" ($n^{/>}c$) is somewhat more difficult to assess. This is mainly because peak capacity is an ill-defined parameter for MS. It is related to the resolving power and, consequently, heavily dependent on the instrumental characteristics. Therefore, we can only estimate the theoretical limits of the peak capacities of MS separation, while again considering the degree of orthogonality with the other techniques.

For given $m/z$ range of 350–950 (a typical range for lipids) the average resolving power in our study, $R_P$ ($m/\Delta m$, FWHM) was ≈14,200. This value gives just a total number of points that may be recorded, not taking into account that only a fraction of the masses is possible and that one compound may generate multiple peaks due to isotopes and fragments, occupying a larger fraction of the separation space. Taking these latter two factors into account, a formula derived for calculating the peak capacity for proteins [92] was used in our study.

This yields approximately

$$n_{MS} = \frac{\frac{R_P}{m}(0.00019m + 0.074)}{(0.001m + 2.05)} \quad (6)$$

where $R_P$ is the average resolving power and $m$ is a given $m/z$ range.

The correlation between separation mechanisms is also affecting the actual effective area of the 2D separation space ("separability"). Several different strategies may be used to obtain orthogonality metrics and to correct estimated peak capacities [93–95].

In the present study we estimated the "indicative separation power" or "separability" in a straightforward manner by multiplying the obtained "asterisk" value ($A_0$) [87] with the maximum theoretical peak capacity. The asterisk value is not a direct measure of the fraction of the separation space covered, but it is thought to provide a reasonable (relative) indication of the effect of the orthogonality on the possible peak capacities for the combined separation approaches.

Thus, the indicative separation power was calculated by modifying Eq. (2) as follows

$$n_{c,12} = n^{/>}c \times n^{/>}c \times [A_0]_{12} \quad (7)$$

For a two-dimensional separation. For a three-dimension separation we may write

$$n_{c,123} = \left(n^{/>}c \times n^{/>}c \times n^{/>}c \times [A_0]_{123}\right) = \left(n^{/>}c \times n^{/>}c \times n^{/>}c \times [A_0]_{12} \times [A_0]_{23} \times [A_0]_{13}\right) \quad (8)$$

where the $n_c$ values are the calculated theoretical peak capacities for the RP ($n^{/>}c$), HILIC or TIMS ($n^{/>}c$) and MS ($n^{/>}c$) dimensions and $A_0$ values indicate the calculates asterisk values between the first and second $[A_0]_{12}$, the second and third $[A_0]_{23}$, and the first and third $[A_0]_{13}$ dimensions, respectively.

A summary of calculated evaluation parameters is provided in Table 2. Assuming identical resolution of MS as third-stage separation after either LC-TIMS or LC × LC (*i.e.* an identical peak capacity of 1038 according to Eq. (7)), the LC-TIMS–MS approach provided a theoretical peak capacity that was about twofold higher than that obtained with LC × LC–MS. The comparably lower values for LC × LC could be mainly attributed to the lower second-dimension (HILIC) peak capacity, which provides the necessary class-type selectivity, but also relatively broad peaks. Nevertheless, adding HILIC as a separation dimension between RPLC and MS (RPLC × HILIC-MS) still represents a considerable gain in peak capacity in comparison with conventional RP-MS, in the same analysis time.

The effects of extra-column band broadening and undersampling contribute heavily to the overall multi-dimensional resolution in the RP × HILIC separation [96,97]. According to Horie et al. [97], and to Vivó Truols et al. [98,99], the optimal modulation rate is approximately 2.5–3 cuts per previous-dimension peak. The sampling time in the LC × LC experiment was 1 min and the average width of the first-dimension peaks about 2 min, resulting in a peak-capacity loss of at least 30%. The rapid gas-phase separation technology of TIMS incorporated as a second dimension allows a twice higher sampling rate than seen in LC × LC. The optimized TIMS duty cycle in this study was 30 s, giving rise to 10% loss due to undersampling. Interestingly, the indicative separation power, based on peak capacity values corrected for orthogonality, was ultimately comparable for the two techniques (see Table 2).

These findings indicate that despite the greater resolving power of the LC-TIMS–MS separation, the high correlation between the TIMS and MS stages results in only 29% orthogonality indicating poor use of the separation space, limiting the overall resolution power.

Additionally, Fig. S5 illustrates the significant influence of the sample solvent arising from the first dimension on the second-dimension separation in LC × LC. In our case, a 20-μL effluent fraction that contained a considerable amount of the strong solvent (2-propanol) led to a serious distortion of the early eluting peaks from the second dimension (*e.g.* TG, Cer, DG, PG) and a concomitant loss of peak capacity. Because of the elimination of the solvent before the gas-phase second dimension in the LC-TIMS–MS approach, the dilution and the strength of the solvent become irrelevant. However, the choice of solvents and, especially, mobile-phase additives is more restricted.

## 4. Conclusions

The analysis of lipid compositions in samples of the complexity of human plasma requires improved separation techniques offer-

**Table 2**
Estimates of the separation potential for various two-dimensional techniques and for the two multidimensional separation techniques studied (LC × LC–MS and LC-TIMS–MS).

| | Analysis/cycle duration (min) | Theoretical peak capacity | Practical peak capacity[a] | Degree of orthogonality [$A_0$][b], % | Separation power[c] |
|---|---|---|---|---|---|
| *RP × HILIC* | 190 | 800 | 576 | 44 | 254 |
| *RP-TIMS* | 190 | 1100 | 991 | 64 | 634 |
| *RP-MS* | 190 | $1.04 \times 10^5$ | $1.04 \times 10^5$ | 69 | $7.16 \times 10^4$ |
| *HILIC-MS* | 1 | 8304 | 8297 | 58 | 4812 |
| *TIMS-MS* | 0.5 | 11418 | 11347 | 29 | 3291 |
| ***RP-TIMS-MS*** | *190* | $1.14 \times 10^6$ | $1.03 \times 10^6$ | *13* | $1.3 \times 10^5$ |
| ***RP × HILIC-MS*** | *190* | $8.30 \times 10^5$ | $5.98 \times 10^5$ | *18* | $1.1 \times 10^5$ |

[a] Corrected for undersampling (according to Eq. (3)).
[b] Evaluated using the asterisk approach [87].
[c] Indicative separation power, taking into account the degree of orthogonality, calculated according to Eq. (6).

ing increased resolution and peak capacity, while maintaining a reasonable analysis time. Two complementary multidimensional techniques, *i.e.* LC-TIMS–MS and LC × LC–MS were investigated in the current study. Both methods were optimized in terms of the comprehensive separation of the major lipid classes and both may be applied for lipidomic analysis.

A slightly higher number of molecular features were found with the LC × LC–MS method (1100) than with LC-TIMS–MS (800), using identical integration parameters, although visually a high number of peaks was observed in the RP-TIMS-MS chromatogram. The latter can be explained by one of the major complications of IMS-based separation. A number of different adducts produced by ESI source will be encountered in both multidimensional approaches. However, in ion-mobility-based separations the adducts are spread across the entire mobilogram, even if that are stemmed from essentially one compound. This may allow the confirmation of lipid-species assignments with a higher certainty, but makes the identification process more laborious. In this context, the interpretation of LC × LC–MS data is more straightforward.

Because of the higher sampling rate of TIMS, the LC-TIMS–MS approach theoretically has a greater separation potential (higher peak capacity by about an order of magnitude). However, due to the high correlation of the TIMS and MS dimensions, the so-called "useful peak capacity" (or "indicative separation power") may ultimately be limited. These two aspects may explain the smaller number of lipids identified by LC-TIMS–MS (55) than by LC × LC–MS (100) in the present study.

Visualization of LC × LC–MS data still remains a challenge, as not all detected ions are apparent, due to great differences in relative ion-intensities. Thus, when there is interest in discovering low-abundance analytes, the visual representation of the raw LC × LC data may lead one to considerably underestimate the power of this technique.

The total analysis time of the separations developed in this study were sub-optimal from an LC–MS and LC-IMS perspective. Much faster separations (within, say, 10 or 20 min) may be performed by LC-IMS–MS [12,100]. Therefore, if the time of analysis is of critical importance, LC-TIMS–MS may be the preferred approach, unless the analysis time in LC × LC can be drastically reduced [101].

One of the major disadvantages of the LC × LC method is poor detection sensitivity resulting from the dilution caused by two successive chromatographic steps, as well as by eventual splitting of the second-dimension effluent prior to the detector. Several remedies have been suggested to overcome the detection-sensitivity limitations [101,102]. The IMS (gas-phase) separation is also affected by diffusion-based band broadening, initial gate pulse width, and instrumental parameters, such as field homogeneity, that may significantly affect the detection limits and the overall resolving power [103]. Because of the limited sensitivity of LC × LC–MS, as well as of the TIMS-MS (prototype) instrument, due to a low trapping efficiency, a considerable amount of the plasma sample was injected in our study. Therefore, the sensitivity aspect was not examined here.

The two three-dimensional methodologies are competing in terms of selectivity and in providing general information about the sample. Because TIMS is a gas-phase separation technique that follows an ionization process, it does not have the capability to remove interfering matrix compounds and to reduce ionization-suppression effects. Improving the separation of co-eluting chromatographic peaks, as done in LC × LC, increases the number of correctly annotated molecular features.

The greatest benefits of the LC-TIMS–MS approach may be achieved for the structural characterization of the sample through separating lipid isomers. The additional information provided by ion-mobility spectrometry – the accurate $K_0$ and CCS values, related to the size and shape of compounds – may aid in confirming lipid identity.

For the high-throughput analysis of large series of complex samples an attractive alternative would be to combine both techniques, performing an untargeted study of the major components by LC × LC and optimizing TIMS for more-detailed structural characterization of compounds of interest. This approach has been recently developed by Stephan et al. [104] for the analysis of a plant extract. The obtained total peak capacity of 8700 by merging two techniques was impressive. However, for simplicity of data interpretation, a modulation time of 4 min was used, sampling entire peaks eluting from the first dimension to the second one. Therefore, the full separation power of LC × LC was not realized. Coupling two techniques (RP × HILIC-TIMS-MS) based on the optimization performed in our study, suggests that a peak capacity of roughly $8.3 \times 10^5$ may be achieved.

No single untargeted method exists today that can cover the full range of lipid features with all their chemical and structural diversity. The two techniques explored in this study are not interchangeable, but may be effectively used in complementary fashion. However, their use seems to be limited at the moment due to a lack of appropriate data-interpretation strategies for multi-dimensional separations.

## Acknowledgements

This research received funding from The Netherlands Organization for Scientific Research (NWO) in the framework of the Technology Area COAST program (HYPERfomance LC project; 053.21.102). We are grateful to Martin Giera and Rico J. E. Derks (Biomolecular Mass Spectrometry Unit, Department of Parasitology, Leiden University Medical Center, Leiden, The Netherlands) and Hyung L. Elfrink (Netherlands Metabolomics Centre, Leiden University) for their support in data interpretation. The authors thank Tim Hoolsteens (DSM Resolve), Robin Sikkens (Vrije University of Amsterdam) and Magdalene Reinkensmeier, Peter Sander and Mark Ridgeway (Bruker Daltonics, Bremen, Germany) for their

support and valuable input. Additionally, the authors like to thank Interreg V_A Euregion Maas-Rijn, province of Limburg (NL), and the department of Economic Affairs in the Netherlands (EUR lipids and Enabling Technology). Andrea Gargano acknowledges the NWO-VENI grant (722.015.009) for the IPA project.

## Appendix A. Supplementary data

Supplementary data associated with this article can be found, in the online version, at https://doi.org/10.1016/j.chroma.2017.11.014.

## References

[1] M.R. Wenk, The emerging field of lipidomics, Nat. Rev. Drug Discov. 4 (2005) 594–610, http://dx.doi.org/10.1038/nrd1776.
[2] D. Steinberg, An interpretive history of the cholesterol controversy: part II: the early evidence linking hypercholesterolemia to coronary disease in humans 1, J. Lipid Res. 46 (2005), http://dx.doi.org/10.1194/jlr.R400012-JLR200.
[3] A.D. Watson, Thematic review series: systems biology approaches to metabolic and cardiovascular disorders. Lipidomics: a global approach to lipid analysis in biological systems, J. Lipid Res. 47 (2006) 2101–2111, http://dx.doi.org/10.1194/jlr.R600022-JLR200.
[4] D.G. McLaren, P.L. Miller, M.E. Lassman, J.M. Castro-Perez, B.K. Hubbard, T.P. Roddy, An ultraperformance liquid chromatography method for the normal-phase separation of lipids, Anal. Biochem. 414 (2011) 266–272, http://dx.doi.org/10.1016/j.ab.2011.03.009.
[5] C.W.N. Damen, G. Isaac, J. Langridge, T. Hankemeier, R.J. Vreeken, Enhanced lipid isomer separation in human plasma using reversed-phase UPLC with ion-mobility/high-resolution MS detection, J. Lipid Res. 55 (2014) 1772–1783, http://dx.doi.org/10.1194/jlr.D047795.
[6] P. Deng, D. Zhong, X. Wang, Y. Dai, L. Zhou, Y. Leng, X. Chen, Analysis of diacylglycerols by ultra performance liquid chromatography-quadrupole time-of-flight mass spectrometry: double bond location and isomers separation, Anal. Chim. Acta 925 (2016) 23–33, http://dx.doi.org/10.1016/j.aca.2016.04.051.
[7] J.F. Brouwers, Liquid chromatographic–mass spectrometric analysis of phospholipids. Chromatography, ionization and quantification, Biochim. Biophys. Acta – Mol. Cell Biol. Lipids 1811 (2011) 763–775, http://dx.doi.org/10.1016/j.bbalip.2011.08.001.
[8] S.N. Jackson, M. Ugarov, J.D. Post, T. Egan, D. Langlais, J.A. Schultz, A.S. Woods, A study of phospholipids by ion mobility TOFMS, J. Am. Soc. Mass Spectrom. 19 (2008) 1655–1662, http://dx.doi.org/10.1016/j.jasms.2008.07.005.
[9] H.I. Kim, H. Kim, E.S. Pang, E.K. Ryu, L.W. Beegle, J.A. Loo, W.A. Goddard, I. Kanik, Structural characterization of unsaturated phosphatidylcholines using traveling wave ion mobility spectrometry, Anal. Chem. 81 (2009) 8289–8297, http://dx.doi.org/10.1021/ac900672a.
[10] L.S. Fenn, M. Kliman, A. Mahsut, S.R. Zhao, J.A. McLean, Characterizing ion mobility-mass spectrometry conformation space for the analysis of complex biological samples, Anal. Bioanal. Chem. 394 (2009) 235–244, http://dx.doi.org/10.1007/s00216-009-2666-3.
[11] T.P.I. Lintonen, P.R.S. Baker, M. Suoniemi, B.K. Ubhi, K.M. Koistinen, E. Duchoslav, J.L. Campbell, K. Ekroos, A.B. Sciex, F.V. Drive, Differential Mobility Spectrometry-Driven Shotgun Lipidomics, 2014.
[12] C.W.N. Damen, G. Isaac, J. Langridge, T. Hankemeier, R.J. Vreeken, Enhanced lipid isomer separation in human plasma using reversed-phase UPLC with ion-mobility/high-resolution MS detection, J. Lipid Res. 55 (2014) 1772–1783, http://dx.doi.org/10.1194/jlr.D047795.
[13] J. Castro-Perez, T.P. Roddy, N.M.M. Nibbering, V. Shah, D.G. McLaren, S. Previs, A.B. Attygalle, K. Herath, Z. Chen, S.-P. Wang, L. Mitnaul, B.K. Hubbard, R.J. Vreeken, D.G. Johns, T. Hankemeier, Localization of fatty acyl and double bond positions in phosphatidylcholines using a dual stage CID fragmentation coupled with ion mobility mass spectrometry, J. Am. Soc. Mass Spectrom. 22 (2011) 1552–1567, http://dx.doi.org/10.1007/s13361-011-0172-2.
[14] V. Shah, J.M. Castro-Perez, D.G. McLaren, K.B. Herath, S.F. Previs, T.P. Roddy, Enhanced data-independent analysis of lipids using ion mobility-TOFMS E to unravel quantitative and qualitative information in human plasma, Rapid Commun, Mass Spectrom. 27 (2013) 2195–2200, http://dx.doi.org/10.1002/rcm.6675.
[15] V. Shah, J.M. Castro-Perez, D.G. McLaren, K.B. Herath, S.F. Previs, T.P. Roddy, Enhanced data-independent analysis of lipids using ion mobility-TOFMS $^{E}$ to unravel quantitative and qualitative information in human plasma, Rapid Commun, Mass Spectrom. 27 (2013) 2195–2200, http://dx.doi.org/10.1002/rcm.6675.
[16] J.E. Kyle, X. Zhang, K.K. Weitz, M.E. Monroe, Y.M. Ibrahim, R.J. Moore, J. Cha, X. Sun, E.S. Lovelace, J. Wagoner, S.J. Polyak, T.O. Metz, S.K. Dey, R.D. Smith, K.E. Burnum-Johnson, E.S. Baker, Uncovering biologically significant lipid isomers with liquid chromatography, ion mobility spectrometry and mass spectrometry, Analyst 141 (2016) 1649–1659, http://dx.doi.org/10.1039/c5an02062j.
[17] A.T. Maccarone, J. Duldig, T.W. Mitchell, S.J. Blanksby, E. Duchoslav, J.L. Campbell, Characterization of acyl chain position in unsaturated phosphatidylcholines using differential mobility-mass spectrometry, J. Lipid Res. 55 (2014) 1668–1677, http://dx.doi.org/10.1194/jlr.M046995.
[18] M. Groessl, S. Graf, R. Knochenmuss, High resolution ion mobility-mass spectrometry for separation and identification of isomeric lipids, Analyst 140 (2015) 6904–6911, http://dx.doi.org/10.1039/C5AN00838G.
[19] J. Castro-Perez, T.P. Roddy, N.M.M. Nibbering, V. Shah, D.G. McLaren, S. Previs, A.B. Attygalle, K. Herath, Z. Chen, S.-P. Wang, L. Mitnaul, B.K. Hubbard, R.J. Vreeken, D.G. Johns, T. Hankemeier, Localization of fatty acyl and double bond positions in phosphatidylcholines using a dual stage CID fragmentation coupled with ion mobility mass spectrometry, J. Am. Soc. Mass Spectrom. 22 (2011) 1552–1567, http://dx.doi.org/10.1007/s13361-011-0172-2.
[20] J.E. Kyle, X. Zhang, K.K. Weitz, M.E. Monroe, Y.M. Ibrahim, R.J. Moore, J. Cha, X. Sun, E.S. Lovelace, J. Wagoner, S.J. Polyak, T.O. Metz, S.K. Dey, R.D. Smith, K.E. Burnum-Johnson, E.S. Baker, Uncovering biologically significant lipid isomers with liquid chromatography, ion mobility spectrometry and mass spectrometry, Analyst 141 (2016) 1649–1659, http://dx.doi.org/10.1039/C5AN02062J.
[21] J.C. May, C.R. Goodwin, N.M. Lareau, K.L. Leaptrot, C.B. Morris, R.T. Kurulugama, A. Mordehai, C. Klein, W. Barry, E. Darland, G. Overney, K. Imatani, G.C. Stafford, J.C. Fjeldsted, J.A. Mclean, Conformational ordering of biomolecules in the gas phase: nitrogen collision cross sections measured on a prototype high resolution drift tube ion mobility-Mass spectrometer, Anal. Chem. 86 (2014) 2107–2116, http://dx.doi.org/10.1021/ac4038448.
[22] G. Paglia, P. Angel, J.P. Williams, K. Richardson, H.J. Olivos, J.W. Thompson, L. Menikarachchi, S. Lai, C. Walsh, A. Moseley, R.S. Plumb, D.F. Grant, B.O. Palsson, J. Langridge, S. Geromanos, G. Astarita, Ion mobility-derived collision cross section as an additional measure for lipid fingerprinting and identification, Anal. Chem. 87 (2015) 1137–1144, http://dx.doi.org/10.1021/ac503715v.
[23] A.A. Shvartsburg, G. Isaac, N. Leveque, R.D. Smith, T.O. Metz, Separation and classification of lipids using differential ion mobility spectrometry, J. Am. Soc. Mass Spectrom. 22 (2011) 1146–1155, http://dx.doi.org/10.1007/s13361-011-0114-z.
[24] P.R.S. Baker, A.M. Armando, J.L. Campbell, O. Quehenberger, E.A. Dennis, Three-dimensional enhanced lipidomics analysis combining UPLC, differential ion mobility spectrometry, and mass spectrometric separation strategies, J. Lipid Res. 55 (2014) 2432–2442, http://dx.doi.org/10.1194/jlr.D051581.
[25] K. Michelmann, J.A. Silveira, M.E. Ridgeway, M.A. Park, Fundamentals of trapped ion mobility spectrometry, J. Am. Soc. Mass Spectrom. 26 (2015) 14–24, http://dx.doi.org/10.1007/s13361-014-0999-4.
[26] F. Fernandez-Lima, D.A. Kaplan, J. Suetering, M.A. Park, Gas-phase separation using a trapped ion mobility spectrometer, Int. J. Ion Mobil. Spectrom. 14 (2011) 93–98, http://dx.doi.org/10.1007/s12127-011-0067-8.
[27] D.R. Hernandez, J.D. DeBord, M.E. Ridgeway, D.A. Kaplan, M.A. Park, F. Fernandez-Lima, Ion dynamics in a trapped ion mobility spectrometer, Analyst 139 (2014) 1913, http://dx.doi.org/10.1039/c3an02174b.
[28] J.A. Silveira, W. Danielson, M.E. Ridgeway, M.A. Park, Altering the mobility-time continuum: nonlinear scan functions for targeted high resolution trapped ion mobility-mass spectrometry, Int. J. Ion Mobility Spectrom. (2016) 1–8, http://dx.doi.org/10.1007/s12127-016-0196-1.
[29] J.A. Silveira, M.E. Ridgeway, M.A. Park, High resolution trapped ion mobility spectrometery of peptides, Anal. Chem. 86 (2014) 5624–5627, http://dx.doi.org/10.1021/ac501261h.
[30] P. Benigni, F. Fernandez-Lima, Oversampling selective accumulation trapped ion mobility spectrometry coupled to FT-ICR MS: fundamentals and applications, Anal. Chem. 88 (2016) 7404–7412, http://dx.doi.org/10.1021/acs.analchem.6b01946.
[31] K.J. Adams, D. Montero, D. Aga, F. Fernandez-Lima, Isomer separation of polybrominated diphenyl ether metabolites using nanoESI-TIMS-MS, Int. J. Ion Mobil. Spectrom. (2016) 1–8, http://dx.doi.org/10.1007/s12127-016-0198-z.
[32] P. Benigni, R. Marin, F. Fernandez-Lima, Towards unsupervised polyaromatic hydrocarbons structural assignment from SA-TIMS–FTMS data, Int. J. Ion Mobility Spectrom. 18 (2015) 151–157, http://dx.doi.org/10.1007/s12127-015-0175-y.
[33] A. Castellanos, P. Benigni, D.R. Hernandez, J.D. DeBord, M.E. Ridgeway, M.A. Park, F. Fernandez-Lima, Fast screening of polycyclic aromatic hydrocarbons using trapped ion mobility spectrometry–mass spectrometry, Anal. Methods 6 (2014) 9328–9332, http://dx.doi.org/10.1039/C4AY01655F.
[34] E.R. Schenk, V. Mendez, J.T. Landrum, M.E. Ridgeway, M.A. Park, F. Fernandez-Lima, Direct observation of differences of carotenoid polyene chain cis/trans isomers resulting from structural topology, Anal. Chem. 86 (2014) 2019–2024, http://dx.doi.org/10.1021/ac403153m.
[35] M.E. Ridgeway, J.A. Silveira, J.E. Meier, Park, Microheterogeneity within conformational states of ubiquitin revealed by high resolution trapped ion mobility spectrometry, Analyst 140 (2015) 6964–6972, http://dx.doi.org/10.1039/C5AN00841G.
[36] E.R. Schenk, R. Almeida, J. Miksovska, M.E. Ridgeway, M.A. Park, F. Fernandez-Lima, Kinetic intermediates of holo- and apo-myoglobin studied using HDX-TIMS-MS and molecular dynamic simulations, J. Am. Soc. Mass Spectrom. 26 (2015) 555–563, http://dx.doi.org/10.1007/s13361-014-1067-9.

[37] P. Benigni, R. Marin, J.C. Molano-Arevalo, A. Garabedian, J.J. Wolff, M.E. Ridgeway, M.A. Park, F. Fernandez-Lima, Towards the analysis of high molecular weight proteins and protein complexes using TIMS-MS, Int. J. Ion Mobility Spectrom. (2016) 1–10, http://dx.doi.org/10.1007/s12127-016-0201-8.
[38] F.A. Fernandez-Lima, D.A. Kaplan, M.A. Park, Note: integration of trapped ion mobility spectrometry with mass spectrometry. Design and optimization of a corona discharge ionization source for ion mobility spectrometry, Rev. Sci. Instrum. 82 (2011) 126106–131570, http://dx.doi.org/10.1063/1.3665933.
[39] M.E. Ridgeway, J.J. Wolff, J.A. Silveira, C. Lin, C.E. Costello, M.A. Park, Gated trapped ion mobility spectrometry coupled to fourier transform ion cyclotron resonance mass spectrometry, Int. J. Ion Mobility Spectrom. (2016) 1–9, http://dx.doi.org/10.1007/s12127-016-0197-0.
[40] P. Benigni, C.J. Thompson, M.E. Ridgeway, M.A. Park, F. Fernandez-Lima, Targeted high-resolution ion mobility separation coupled to ultrahigh-resolution mass spectrometry of endocrine disruptors in complex mixtures, Anal. Chem. 87 (2015) 4321–4325, http://dx.doi.org/10.1021/ac504866v.
[41] A. McKenzie-Coe, J.D. DeBord, M. Ridgeway, M. Park, G. Eiceman, F. Fernandez-Lima, Lifetimes and stabilities of familiar explosive molecular adduct complexes during ion mobility measurements, Analyst 140 (2015) 5692–5699, http://dx.doi.org/10.1039/C5AN00527B.
[42] K. Sandra, A.D.S. Pereira, G. Vanhoenacker, F. David, P. Sandra, Comprehensive blood plasma lipidomics by liquid chromatography/quadrupole time-of-flight mass spectrometry, J. Chromatogr. A 1217 (2010) 4087–4099, http://dx.doi.org/10.1016/j.chroma.2010.02.039.
[43] R. T'Kindt, L. Jorge, E. Dumont, P. Couturon, F. David, P. Sandra, K. Sandra, Profiling and characterizing skin ceramides using reversed-phase liquid chromatography-quadrupole time-of-flight mass spectrometry, Anal. Chem. 84 (2012) 403–411, http://dx.doi.org/10.1021/ac202646v.
[44] J.M. Castro-Perez, J. Kamphorst, J. Degroot, F. Lafeber, J. Goshawk, K. Yu, J.P. Shockcor, R.J. Vreeken, T. Hankemeier, Comprehensive LC-MSE lipidomic analysis using a shotgun approach and its application to biomarker detection and identification in osteoarthritis patients, J. Proteome Res. 9 (2010) 2377–2389, http://dx.doi.org/10.1021/pr901094j.
[45] T. Cajka, O. Fiehn, Comprehensive analysis of lipids in biological systems by liquid chromatography-mass spectrometry, TrAC – Trends Anal. Chem. 61 (2014) 192–206, http://dx.doi.org/10.1016/j.trac.2014.04.017.
[46] E. Sokol, R. Almeida, H.K. Hannibal-Bach, D. Kotowska, J. Vogt, J. Baumgart, K. Kristiansen, R. Nitsch, J. Knudsen, C.S. Ejsing, Profiling of lipid species by normal-phase liquid chromatography, nanoelectrospray ionization, and ion trap–orbitrap mass spectrometry, Anal. Biochem. 443 (2013) 88–96, http://dx.doi.org/10.1016/j.ab.2013.08.020.
[47] S. Harrabi, W. Herchi, H. Kallel, P.M. Mayer, S. Boukhchina, Liquid chromatographic–mass spectrometric analysis of glycerophospholipids in corn oil, Food Chem. 114 (2009) 712–716, http://dx.doi.org/10.1016/j.foodchem.2008.09.092.
[48] P.M. Hutchins, R.M. Barkley, R.C. Murphy, Separation of cellular nonpolar neutral lipids by normal-phase chromatography and analysis by electrospray ionization mass spectrometry, J. Lipid Res. 49 (2008) 804–813, http://dx.doi.org/10.1194/jlr.M700521-JLR200.
[49] L. Norlén, I. Nicander, A. Lundsjö, T. Cronholm, B. Forslind, A new HPLC-based method for the quantitative analysis of inner stratum corneum lipids with special reference to the free fatty acid fraction, Arch. Dermatol. Res. 290 (1998) 508–516, http://dx.doi.org/10.1007/s004030050344.
[50] J. van Smeden, L. Hoppel, R. van der Heijden, T. Hankemeier, R.J. Vreeken, J. a Bouwstra, LC/MS analysis of stratum corneum lipids: ceramide profiling and discovery, J. Lipid Res. 52 (2011) 1211–1221, http://dx.doi.org/10.1194/jlr.M014456.
[51] P. Česla, J. Křenková, Fraction transfer process in on-line comprehensive two-dimensional liquid-phase separations, J. Sep. Sci. 40 (2017) 109–123, http://dx.doi.org/10.1002/jssc.201600921.
[52] M. Lísa, E. Cífková, M. Holčapek, Lipidomic profiling of biological tissues using off-line two-dimensional high-performance liquid chromatography-mass spectrometry, J. Chromatogr. A 1218 (2011) 5146–5156, http://dx.doi.org/10.1016/j.chroma.2011.05.081.
[53] H. Nie, R. Liu, Y. Yang, Y. Bai, Y. Guan, D. Qian, T. Wang, H. Liu, Lipid profiling of rat peritoneal surface layers by online normal- and reversed-phase 2D LC QToF-MS, J. Lipid Res. 51 (2010) 2833–28444, http://dx.doi.org/10.1194/jlr.D007567.
[54] M. Li, X. Tong, P. Lv, B. Feng, L. Yang, Z. Wu, X. Cui, Y. Bai, Y. Huang, H. Liu, A not-stop-flow online normal-/reversed-phase two-dimensional liquid chromatography-quadrupole time-of-flight mass spectrometry method for comprehensive lipid profiling of human plasma from atherosclerosis patients, J. Chromatogr. A 1372C (2014) 110–119, http://dx.doi.org/10.1016/j.chroma.2014.10.094.
[55] H.C. Van De Ven, A.F.G. Gargano, S. Van Der Wal, P.J. Schoenmakers, Switching solvent and enhancing analyte concentrations in small effluent fractions using in-column focusing, J. Chromatogr. A 1427 (2016) 90–95.
[56] R.J. Vonk, A.F.G. Gargano, E. Davydova, H.L. Dekker, S. Eeltink, L.J. de Koning, P.J. Schoenmakers, Comprehensive two-dimensional liquid chromatography with stationary-phase-assisted modulation coupled to high-resolution mass spectrometry applied to proteome analysis of *Saccharomyces cerevisiae*, Anal. Chem. 87 (2015) 5387–5394, http://dx.doi.org/10.1021/acs.analchem.5b00708.
[57] Z. Guan, J. Grünler, S. Piao, P.J. Sindelar, Separation and quantitation of phospholipids and their ether analogues by high-performance liquid chromatography, Anal. Biochem. 297 (2001) 137–143, http://dx.doi.org/10.1006/abio.2001.5303.
[58] B.L. Peterson, B.S. Cummings, A review of chromatographic methods for the assessment of phospholipids in biological samples, Biomed. Chromatogr. 20 (2006) 227–243, http://dx.doi.org/10.1002/bmc.563.
[59] S. Wang, J. Li, X. Shi, L. Qiao, X. Lu, G. Xu, A novel stop-flow two-dimensional liquid chromatography-mass spectrometry method for lipid analysis, J. Chromatogr. A 1321 (2013) 65–72, http://dx.doi.org/10.1016/j.chroma.2013.10.069.
[60] P. Dugo, N. Fawzy, F. Cichello, F. Cacciola, P. Donato, L. Mondello, Stop-flow comprehensive two-dimensional liquid chromatography combined with mass spectrometric detection for phospholipid analysis, J. Chromatogr. A 1278 (2013) 46–53, http://dx.doi.org/10.1016/j.chroma.2012.12.042.
[61] C. Sun, Y.-Y. Zhao, J.M. Curtis, Elucidation of phosphatidylcholine isomers using two dimensional liquid chromatography coupled in-line with ozonolysis mass spectrometry, J. Chromatogr. A 1351 (2014) 37–45, http://dx.doi.org/10.1016/j.chroma.2014.04.069.
[62] M. Narváez-Rivas, N. Vu, G.-Y. Chen, Q. Zhang, Off-line mixed-mode liquid chromatography coupled with reversed phase high performance liquid chromatography-high resolution mass spectrometry to improve coverage in lipidomics analysis, Anal. Chim. Acta 954 (2017) 140–150, http://dx.doi.org/10.1016/j.aca.2016.12.003.
[63] M. Holčapek, M. Ovčačíková, M. Lísa, E. Cífková, T. Hájek, Continuous comprehensive two-dimensional liquid chromatography-electrospray ionization mass spectrometry of complex lipidomic samples, Anal. Bioanal. Chem. 407 (2015) 5033–5043, http://dx.doi.org/10.1007/s00216-015-8528-2.
[64] J. Folch, M. Lees, G.H.S. Stanley, A simple method for the isolation and purification of total lipids from animal tissues, J. Biol. Chem. 226 (1957) 497–509, http://dx.doi.org/10.1007/s10858-011-9570-9.
[65] S.K. Byeon, J.Y. Lee, M.H. Moon, Optimized extraction of phospholipids and lysophospholipids for nanoflow liquid chromatography-electrospray ionization-tandem mass spectrometry, Analyst 137 (2012) 451, http://dx.doi.org/10.1039/c1an15920h.
[66] M.O.T. Pluskal, S. Castillo, A. Villar-Briones, MZmine 2: modular framework for processing, visualizing, and analyzing mass spectrometry-based molecular profile data, BMC Bioinf. 11 (2010) 318–328, http://dx.doi.org/10.1186/1471-2105-11-395.
[67] M. Katajamaa, J. Miettinen, M. Oresic, MZmine: toolbox for processing and visualization of mass spectrometry based molecular profile data, Bioinformatics 22 (2006) 634–636, http://dx.doi.org/10.1093/bioinformatics/btk039.
[68] K. Schmelzer, E. Fahy, S. Subramaniam, E.A. Dennis, The lipid maps initiative in lipidomics, Methods Enzymol. 432 (2007) 171–183, http://dx.doi.org/10.1016/S0076-6879(07)32007-7.
[69] S. Wong, M. Ritchie, Methods of separating lipids. U.S. Patent 20140338432 A1, 2014. https://www.google.com/patents/US20140338432#backward-citations. (Accessed 6 March 2017).
[70] J.D. Netto, S. Wong, M. Ritchie, High resolution separation of phospholipids using a novel orthogonal two-dimensional UPLC/QTof MS system configuration, Waters Appl. Note (2013), 720004546. http://www.waters.com/webassets/cms/library/docs/720004546en.pdf. (Accessed 1 August 2017).
[71] C.L. Bowen, J. Kehler, C.A. Evans, Development and validation of a sensitive and selective UHPLC-MS/MS method for simultaneous determination of both free and total eicosapentaeonic acid and docosahexenoic acid in human plasma, J. Chromatogr. B Anal. Technol. Biomed. Life Sci. 878 (2010) 3125–3133, http://dx.doi.org/10.1016/j.jchromb.2010.09.020.
[72] J.M. Castro-Perez, J. Kamphorst, J. DeGroot, F. Lafeber, J. Goshawk, K. Yu, J.P. Shockcor, R.J. Vreeken, T. Hankemeier, Comprehensive LC-MS $^{E}$ lipidomic analysis using a shotgun approach and its application to biomarker detection and identification in osteoarthritis patients, J. Proteome Res. 9 (2010) 2377–2389, http://dx.doi.org/10.1021/pr901094j.
[73] T. Cajka, O. Fiehn, Increasing lipidomic coverage by selecting optimal mobile-phase modifiers in LC–MS of blood plasma, Metabolomics 12 (2016) 34, http://dx.doi.org/10.1007/s11306-015-0929-x.
[74] R. Sikkens, Human Plasma Lipidomics, Identification of Lipid Markers in Cardiovascular Disease Using an Untargeted LC-MS Based Approach, Master's Thesis, Free University of Amsterdam, 2016.
[75] G. Liebisch, J.A. Vizcaíno, H. Köfeler, M. Trötzmüller, W.J. Griffiths, G. Schmitz, F. Spener, M.J.O. Wakelam, Shorthand notation for lipid structures derived from mass spectrometry, J. Lipid Res. 54 (2013) 1523–1530, http://dx.doi.org/10.1194/jlr.M033506.
[76] K.M. Hines, J. Herron, L. Xu, Assessment of altered lipid homeostasis by HILIC-Ion mobility-mass spectrometry-based lipidomics, J. Lipid Res. (2017), http://dx.doi.org/10.1194/jlr.D074724, jlr.D074724.
[77] R.E. Patterson, A.J. Ducrocq, D.J. McDougall, T.J. Garrett, R.A. Yost, Comparison of blood plasma sample preparation methods for combined LC–MS lipidomics and metabolomics, J. Chromatogr. B 1002 (2015) 260–266, http://dx.doi.org/10.1016/j.jchromb.2015.08.018.
[78] Y. Yang, C. Cruickshank, M. Armstrong, S. Mahaffey, R. Reisdorph, N. Reisdorph, New sample preparation approach for mass spectrometry-based profiling of plasma results in improved coverage of metabolome, J.

Chromatogr. A 1300 (2013) 217–226, http://dx.doi.org/10.1016/j.chroma.2013.04.030.
[79] J.C. May, C.R. Goodwin, N.M. Lareau, K.L. Leaptrot, C.B. Morris, R.T. Kurulugama, A. Mordehai, C. Klein, W. Barry, E. Darland, G. Overney, K. Imatani, G.C. Stafford, J.C. Fjeldsted, J.A. Mclean, Conformational ordering of biomolecules in the gas phase: nitrogen collision cross sections measured on a prototype high resolution drift tube ion mobility-mass spectrometer, Anal. Chem. 86 (2015) 2107–2116, http://dx.doi.org/10.1021/ac4038448.
[80] G. Paglia, P. Angel, J.P. Williams, K. Richardson, H.J. Olivos, J.W. Thompson, L. Menikarachchi, S. Lai, C. Walsh, A. Moseley, R.S. Plumb, D.F. Grant, B.O. Palsson, J. Langridge, S. Geromanos, G. Astarita, Ion mobility-derived collision cross section as an additional measure for lipid fingerprinting and identification, Anal. Chem. 87 (2015) 1137–1144, http://dx.doi.org/10.1021/ac503715v.
[81] K.M. Hines, J.C. May, J.A. Mclean, L. Xu, Evaluation of collision cross section calibrants for structural analysis of lipids by traveling wave ion mobility-mass spectrometry, Anal. Chem. 88 (2016) 7329–7336, http://dx.doi.org/10.1021/acs.analchem.6b01728.
[82] W.B. Ridenour, M. Kliman, J.A. McLean, R.M. Caprioli, Structural characterization of phospholipids and peptides directly from tissue sections by MALDI traveling-wave ion mobility-mass spectrometry, Anal. Chem. 82 (2010) 1881–1889, http://dx.doi.org/10.1021/ac9026115.
[83] M. Beccaria, V. Inferrera, F. Rigano, K. Gorynski, G. Purcaro, J. Pawliszyn, P. Dugo, L. Mondello, Highly informative multiclass profiling of lipids by ultra-high performance liquid chromatography–low resolution (quadrupole) mass spectrometry by using electrospray ionization and atmospheric pressure chemical ionization interfaces, J. Chromatogr. A 1509 (2017) 69–82, http://dx.doi.org/10.1016/j.chroma.2017.06.017.
[84] J.M. Castro-Perez, J. Kamphorst, J. DeGroot, F. Lafeber, J. Goshawk, K. Yu, J.P. Shockcor, R.J. Vreeken, T. Hankemeier, Comprehensive LC-MS $^{E}$ lipidomic analysis using a shotgun approach and its application to biomarker detection and identification in osteoarthritis patients, J. Proteome Res. 9 (2010) 2377–2389, http://dx.doi.org/10.1021/pr901094j.
[85] T.P.I. Lintonen, P.R.S. Baker, M. Suoniemi, B.K. Ubhi, K.M. Koistinen, E. Duchoslav, J.L. Campbell, K. Ekroos, Differential mobility spectrometry-driven shotgun lipidomics, Anal. Chem. 86 (2014) 9662–9669, http://dx.doi.org/10.1021/ac5021744.
[86] M. Kliman, J.C. May, J.A. McLean, Lipid analysis and lipidomics by structurally selective ion mobility-mass spectrometry, Biochim. Biophys. Acta – Mol. Cell Biol. Lipids 2011 (1811) 935–945, http://dx.doi.org/10.1016/j.bbalip.2011.05.016.
[87] M. Camenzuli, P.J. Schoenmakers, A new measure of orthogonality for multi-dimensional chromatography, Anal. Chim. Acta 838 (2014) 93–101, http://dx.doi.org/10.1016/j.aca.2014.05.048.
[88] T.J. Causon, S. Hann, Theoretical evaluation of peak capacity improvements by use of liquid chromatography combined with drift tube ion mobility-mass spectrometry, J. Chromatogr. A 1416 (2015) 47–56, http://dx.doi.org/10.1016/j.chroma.2015.09.009.
[89] E. Davydova, P.J. Schoenmakers, G. Vivó-Truyols, Study on the performance of different types of three-dimensional chromatographic systems, J. Chromatogr. A 1271 (2013) 137–143, http://dx.doi.org/10.1016/j.chroma.2012.11.043.
[90] X. Li, D.R. Stoll, P.W. Carr, Equation for peak capacity estimation in two-dimensional liquid chromatography, Anal. Chem. 81 (2009) 845–850, http://dx.doi.org/10.1021/ac801772u.
[91] B.B. Schneider, T.R. Covey, S.L. Coy, E.V. Krylov, E.G. Nazarov, Chemical effects in the separation process of a differential mobility/mass spectrometer system, Anal. Chem. 82 (2010) 1867–1880, http://dx.doi.org/10.1021/ac902571u.
[92] J.L. Frahm, B.E. Howard, S. Heber, D.C. Muddiman, Accessible proteomics space and its implications for peak capacity for zero-, one- and two-dimensional separations coupled with FT-ICR and TOF mass spectrometry, J. Mass Spectrom. 41 (2006) 281–288, http://dx.doi.org/10.1002/jms.1024.
[93] M.R. Schure, J.M. Davis, Orthogonal separations: comparison of orthogonality metrics by statistical analysis, J. Chromatogr. A 1414 (2015) 60–76, http://dx.doi.org/10.1016/j.chroma.2015.08.029.
[94] M. Gilar, P. Olivova, A.E. Daly, J.C. Gebler, Orthogonality of separation in two-dimensional liquid chromatography, Anal. Chem. 77 (2005) 6426–6434, http://dx.doi.org/10.1021/ac050923i.
[95] Z. Liu, D.G. Patterson, M.L. Lee, Geometric approach to factor analysis for the estimation of orthogonality and practical peak capacity in comprehensive two-dimensional separations, Anal. Chem. 67 (1995) 3840–3845, http://dx.doi.org/10.1021/ac00117a004.
[96] P.J. Schoenmakers, G. Vivó-Truyols, W.M.C. Decrop, A protocol for designing comprehensive two-dimensional liquid chromatography separation systems, J. Chromatogr. A 1120 (2006) 282–290, http://dx.doi.org/10.1016/j.chroma.2005.11.039.
[97] J.M. Davis, D.R. Stoll, P.W. Carr, Effect of first-dimension undersampling on effective peak capacity in comprehensive two-dimensional separations, Anal. Chem. 80 (2008) 461–473, http://dx.doi.org/10.1021/ac071504j.
[98] K. Horie, H. Kimura, T. Ikegami, A. Iwatsuka, N. Saad, O. Fiehn, N. Tanaka, Calculating optimal modulation periods to maximize the peak capacity in two-dimensional HPLC, Anal. Chem. 79 (2007) 3764–3770, http://dx.doi.org/10.1021/AC062002T.
[99] G. Vivoí-Truyols, S. van der Wal, P.J. Schoenmakers, Comprehensive study on the optimization of online two-dimensional liquid chromatographic systems considering losses in theoretical peak capacity in first- and second-dimensions: a pareto-optimality approach, Anal. Chem. 82 (2010) 8525–8536, http://dx.doi.org/10.1021/ac101420f.
[100] G. Paglia, P. Angel, J.P. Williams, K. Richardson, H.J. Olivos, J. Will Thompson, L. Menikarachchi, S. Lai, C. Walsh, A. Moseley, R.S. Plumb, D.F. Grant, B.O. Palsson, J. Langridge, S. Geromanos, G. Astarita, Ion mobility-derived collision cross section as an additional measure for lipid fingerprinting and identification, Anal. Chem. 87 (2015) 1137–1144, http://dx.doi.org/10.1021/ac503715v.
[101] A.F.G. Gargano, M. Duffin, P. Navarro, P.J. Schoenmakers, Reducing dilution and analysis time in online comprehensive two-dimensional liquid chromatography by active modulation, Anal. Chem. 88 (2016) 1785–1793, http://dx.doi.org/10.1021/acs.analchem.5b04051.
[102] D.R. Stoll, P.W. Carr, Two-dimensional liquid chromatography: a state of the art tutorial, Anal. Chem. 89 (2017) 519–531, http://dx.doi.org/10.1021/acs.analchem.6b03506.
[103] A.B. Kanu, M.M. Gribb, H.H. Hill, Predicting optimal resolving power for ambient pressure ion mobility spectrometry, Anal. Chem. 80 (2008) 6610–6619, http://dx.doi.org/10.1021/ac8008143.
[104] S. Stephan, C. Jakob, J. Hippler, O.J. Schmitz, A novel four-dimensional analytical approach for analysis of complex samples, Anal. Bioanal. Chem. (2016) 3751–3759, http://dx.doi.org/10.1007/s00216-016-9460-9.